AD_____

AWARD NUMBER: DAMD17-03-C-0122

TITLE: Novel Therapeutic and Prophylactic Modalities to Protect the United States Armed Forces Against Major Biological Threat Agents

PRINCIPAL INVESTIGATOR: Serguei G. Popov, Ph.D.
Chris Bradburne
Myung-Chul Chung
Bryan Millis
Svetlana Nazarenko
Taissia G. Popova

CONTRACTING ORGANIZATION: George Mason University
Manassas, Virginia 20110

REPORT DATE: October 2005

TYPE OF REPORT: Annual

PREPARED FOR: U.S. Army Medical Research and Materiel Command
Fort Detrick, Maryland 21702-5012

DISTRIBUTION STATEMENT: Approved for Public Release;
Distribution Unlimited

The views, opinions and/or findings contained in this report are those of the author(s) and should not be construed as an official Department of the Army position, policy or decision unless so designated by other documentation.

REPORT DOCUMENTATION PAGE

Form Approved
OMB No. 0704-0188

Public reporting burden for this collection of information is estimated to average 1 hour per response, including the time for reviewing instructions, searching existing data sources, gathering and maintaining the data needed, and completing and reviewing this collection of information. Send comments regarding this burden estimate or any other aspect of this collection of information, including suggestions for reducing this burden to Department of Defense, Washington Headquarters Services, Directorate for Information Operations and Reports (0704-0188), 1215 Jefferson Davis Highway, Suite 1204, Arlington, VA 22202-4302. Respondents should be aware that notwithstanding any other provision of law, no person shall be subject to any penalty for failing to comply with a collection of information if it does not display a currently valid OMB control number. **PLEASE DO NOT RETURN YOUR FORM TO THE ABOVE ADDRESS.**

1. REPORT DATE *(DD-MM-YYYY)*	**2. REPORT TYPE**	**3. DATES COVERED** *(From - To)*
01-10-2005	Annual	29 Sep 2004 – 28 Sep 2005

4. TITLE AND SUBTITLE

Novel Therapeutic and Prophylactic Modalities to Protect the United States Armed Forces Against Major Biological Threat Agents

5a. CONTRACT NUMBER
DAMD17-03-C-0122

5b. GRANT NUMBER

5c. PROGRAM ELEMENT NUMBER

6. AUTHOR(S)
Serguei G. Popov, Ph.D., Chris Bradburne, Myung-Chul Chung, et al.

E-Mail: spopov@gmu.edu

5d. PROJECT NUMBER

5e. TASK NUMBER

5f. WORK UNIT NUMBER

7. PERFORMING ORGANIZATION NAME(S) AND ADDRESS(ES)

George Mason University
Manassas, Virginia 20110

8. PERFORMING ORGANIZATION REPORT NUMBER

9. SPONSORING / MONITORING AGENCY NAME(S) AND ADDRESS(ES)
U.S. Army Medical Research and Materiel Command
Fort Detrick, Maryland 21702-5012

10. SPONSOR/MONITOR'S ACRONYM(S)

11. SPONSOR/MONITOR'S REPORT NUMBER(S)

12. DISTRIBUTION / AVAILABILITY STATEMENT
Approved for Public Release; Distribution Unlimited

13. SUPPLEMENTARY NOTES

14. ABSTRACT

Secreted virulence factors, in addition to lethal toxin (LT), play an important role in anthrax and have previously been identified by us as candidate targets of post-exposure therapies. However, the molecular substrates and specific pathogenic mechanisms of these factors remain largely unknown. During the year 2005, the data generated using epithelial cells in culture and mice challenged with B. anthracis spores allow conclude that acceleration of ectodomain shedding by LT, other proteolytic proteins and hemolysis represents a new previously unknown feature of anthrax infection. Secreted pathogenic factors of B. anthracx can cause ectodomain shedding likely resulting in protective barriers disruption and tissue penetration by bacilli. In addition, proteolysis of the extracellular matrix can play signaling role as a mediator of lethality perturbing different mechanisms of the host defense response, including the activation of TLRs. Data on pharmacological inhibition of shedding favor a hypothesis that activities of tested bacterial shedding inducers converge on the stimulation of cytoplasmic tyrosine kinases of the Syk family, ultimately leading to activation of cellular sheddase. Both LT and pore-forming hemolysin O transiently modulate ERK1/2 and p38 MAPK signaling pathways, while JNK pathway seems to be irrelevant to accelerate shedding. The concerted acceleration of shedding by several virulence factors could represent a pathogenic mechanism, contributing to hemorrhage, edema and abdominal cell signaling during anthrax infection.

15. SUBJECT TERMS
biological weapons, lethal toxin blocker, protease inhibitors, toll-like receptors

16. SECURITY CLASSIFICATION OF:			**17. LIMITATION OF ABSTRACT**	**18. NUMBER OF PAGES**	**19a. NAME OF RESPONSIBLE PERSON**
a. REPORT	**b. ABSTRACT**	**c. THIS PAGE**			USAMRMC
U	U	U	UU	78	**19b. TELEPHONE NUMBER** *(include area code)*

Standard Form 298 (Rev. 8-98)
Prescribed by ANSI Std. Z39.18

Table of Contents

Introduction

Our previous research on this project demonstrated that *B. anthracis* cultivated in culture media secrets a number of proteolytic virulence factors, including those with hemorrhagic, caseinolytic and gelatinolytic activities (Popov *et al.*, 2005). These factors in most respects are distinct from LT, including the mode of their expression under aerobic conditions, their molecular targets, as well as a high virulent potency upon intratracheal administration. Chemical inhibitors of these factors demonstrated a substantial protective efficacy in combination with antibiotic therapy. Our findings outlined a new direction in the development of anthrax therapeutic approaches, and helped close a substantial gap between the understanding of anthrax molecular pathology and the most prominent clinical features of its infectious process. Complexity of the anthrax secretome composition with regard to the number and specificity of proteolytic enzymes suggested a multitude of their potential virulent mechanisms that needed to be explored further.

Current report describes our progress in isolation and characterization of *B. anthracis* proteolytic pathogenic factors. Interestingly, our new data allow suggest that anthrax proteases, including LT, are capable of damaging the host cells through the previously unrecognized anthrax pathogenic mechanism, which includes the host cell ectodomain shedding. In addition to the proteolytic enzymes, the data presented below demonstrate that other pathogenic factors such as hemolysins are also active in the acceleration of shedding. In connection with these observations we report characterization of the isolated anthrax neutral proteases and hemolytic proteins AnlO, AnlB, as well as the AnlA homolog ClnA from *B. cereus*, regarding their heparan sulfate ectodomain shedding and barrier permeability enhancing activities. We found that LT also stimulates shedding by the mechanism which involves the MAPKK signaling pathways. Our preliminary data demonstrate that shedding of syndecan (Synd) ectodomain is relevant to the infectious process in the *B. anthracis* (Sterne) spore-challenged mice. The elevated levels of shed Synd1 and Synd4 are readily detectable in the circulation on the next day after challenge. Our observations identify a novel concerted strategy of anthrax virulence factors influencing different host cell signaling pathways but all ultimately converging on stimulation of ectodomain shedding. This new feature of the anthrax infectious process could be of high pathogenic significance. We

suggest that a cumulative effect of several virulence factors on the acceleration of ectodomain shedding could compromise the integrity of host protective barriers, cause malfunction of major organs and ultimately contribute to the pathological systemic response typical in anthrax patients.

Body of the Report

1. Task 1. Synergistic Anti-Toxin/Antibiotic Treatment Of Anthrax

Experiments on this task have been completed and reported in the year 2004. Recent publications cited below confirm the results obtained within current project and demonstrate that treatment with beta-cyclodextrin derivatives can protect mice challenged with lethal toxin:

Beta-cyclodextrin derivatives that inhibit anthrax lethal toxin. Karginov VA, Yohannes A, Robinson TM, Fahmi NE, Alibek K, Hecht SM. Bioorg Med Chem. 2005; [Epub ahead of print]

Blocking anthrax lethal toxin at the protective antigen channel by using structure-inspired drug design. Karginov VA, Nestorovich EM, Moayeri M, Leppla SH, Bezrukov SM. Proc Natl Acad Sci U S A. 2005;102(42):15075-80.

2. Task 2. Anthrax Protease Inhibitors For Therapy Of Late-Stage Inhalational Anthrax

2.1. Background

It has been recently reported that major pathogens *Staphylococcus aureus* and *Pseudomonas aeruginosa*, exploit acceleration of syndecan (Synd) ectodomain shedding as a mechanism of host damage (Park *et al.*, 2000; Park *et al.*, 2001;Park *et al.*, 2004). Approximately 1% of cell surface proteins are thought to be shed into the extracellular environment by normal host cells (Hooper and Turner, 1999) however during the infectious process shedding can reach pathological proportions. The diverse list of proteins, which are normally shed from the cell surface includes but is not limited to cytokines, growth factors, and cell adhesion molecules, such as tumor necrosis factor (TNFα), transforming growth factor α (TGFα), epidermal growth factors (EGFs), L-

selectin, CD44, and Synds (Fitzgerald *et al.*, 2000 and citations within). Syndecans (Synds) are a group of four distinct proteoglycans (PGs), containing transmembrane core proteins modified with several heparan sulfate (HS) and chondroitin sulfate chains. Synd1 is the major HS PG of epithelial cells, which binds and regulates a wide variety of biological molecules through its HS chains (Beauvais and Rapraeger, 2004). Synds act as adhesion molecules, modulators of growth factor function, and co-receptors in processes as diverse as morphogenesis, tissue repair, host defense, tumor development, and energy metabolism. In mammary epithelial cells Synd1 co-localizes with actin filaments thus anchoring cytoskeleton to extracellular matrix. Synd4 can be found in the focal adhesion junctions between cells (Wilcox-Adelman *et al.*, 2002). Therefore, Synds are involved in modulation of cell spreading, adhesion, motility and maintenance of intercellular contacts. Ectodomain shedding rapidly changes the surface phenotype of affected cells and generates soluble, biologically active ectodomains that can function as paracrine or autocrine effectors. A growing body of evidence indicates that these molecular and cellular features enable ectodomain shedding to regulate many pathophysiological processes, such as microbial pathogenesis, inflammation, and tissue repair (Bernfield *et al.*, 1999; Park *et al.*, 2000).

Shedding of Synds can be abnormally increased in the cause of the infectious process. The *P. aeruginosa* shedding enhancer was identified as LasA, a known metalloprotease virulence factor (Park *et al.*, 2000). Studies *in vivo* indicate that *P. aeruginosa* activates Synd1 shedding to enhance its virulence in a murine model of lung infection (Park *et al.*, 2001). Shedding enhancers of *S. aureus* are represented by pore-forming α-toxin and sphingomyelinase β-toxin (Park *et al.*, 2004). During the infectious process, proteolytic removal of ectodomain in a soluble form by secreted microbial factors could enhance host colonization by altering the morphology and compromising the integrity of protective barriers formed by polarized epithelial cells of the skin, the surfaces of body cavities and internal organs, as well as endothelial cells of the blood vessel walls. The initial pathology can be further aggravated by exposing intercellular, basolateral, and subepithelial adhesive components (Mun-Bryce and Rosenberg, 1998). Structural damage to the host cell surface caused by ectodomain shedding along with pathological signaling may initiate a mechanism ultimately leading to the malfunction and failure of life-critical organs and systems.

Inhalation anthrax is a systemic disease characterized by a severe damage to epithelia residing in major internal organs such as the liver, lung, intestines, spleen and kidneys. Disruption of vasculature resulting in massive hemorrhages and pleural edema is a hallmark of systemic anthrax (Abramova *et al.*, 1993; Grinberg *et al.*, 2001, Vasconcelos *et al.*, 2003). The *B. anthracis* genome contains genes for several proteolytic and hemolytic factors, which are structurally similar to the shedding inducers from *P. aeruginosa* and *S. aureus*, including among others the *S. aureus* α- and β-toxin homologues: anthralysin O (AnlO, pore-forming cholesterol-dependent hemolysin) and anthralysin B (AnlB, sphingomyelienase), respectively (Klichko *et al.*, 2002; Read *et al.*, 2003). Another anthrax hemolytic factor of interest regarding its potential activity in ectodomain shedding is the AnlA (phosphatidyl choline-preferring phospholipase C, PC-PLC), which is 99% homologous to its *B. cereus* counterpart, ClnA (Klichko *et al.,* 2002). Johansen *et al.* (1994) reported that NIH 3T3 cells stably transfected with the gene encoding ClnA displayed a transformed phenotype. Exogenously applied ClnA decreased cell-cell contacts and increased cell migration resulting in disruption of the advancing epithelial sheet in the wound healing process (Firth *et al.*, 2001). Despite of these observations the ectodomain shedding has never been studied with regard to infections caused by *B. anthrasis* or *B. cereus*. Therefore, the main goal of this report was to investigate if Synd ectodomain goal takes place in anthrax, and to test our hypothesis regarding the shedding activity of anthrax hemolytic proteins.

In addition to the hemolytic proteins our attention was attracted to the lethal toxin (LT), a major anthrax virulence factor (Moayeri and Leppla, 2004). The mediator(s) of its toxicity remains unknown. It has been shown that LT abrogates intracellular signaling through proteolytic cleavage of mitogen-activated protein kinase kinases (MAPKK) (Duesbery *et al.*, 1998) resulting in the induction of apoptosis in isolated macrophages stimulated with AnlO (Park *et al.,* 2004). Administration of lethal doses of a purified LT to mice and rats causes pleural edema (Moayeri *et al.*, 2003) indicating that LT compromises the integrity of intercellular contacts maintaining the fluid homeostasis in the lung. It has been previously suggested that LT is capable of increasing vascular permeability (Smith and Stoner, 1967), and recent experiments with endothelial cells in culture are consistent with this conclusion (Warfel *et al.*, 2005). Therefore, we wanted to test

whether LT can function as a shedding inducer, and whether the inhibition of MAPKKs by LT modulates cell signaling relevant to shedding.

2.2. Results

Isolation of proteases

Overall purification of the proteases from *B. anthracis* is summarized in Table 1. The purified proteases showed roughly a 3.18-fold purification rate over the crude culture supernatants. Two major proteins were isolated. The purified enzymes showed a single band of the protein designated P1 with a molecular weight of ~36 kDa and two bands for the protein designated P2 with molecular weight of ~46 and ~18 kDa on reduced SDS-PAGE gel (Fig. 1).

Table 1. Summary of purification of extracellular proteases from *B. anthracis*

Purification Steps	Total Volume	Total Protein	Activity	Total activity	Specific Activity	Recovery	Purification
	ml	*mg*	*U/ml*	*U*	*U/mg*	*%*	*fold*
Culture supernatant	940	1.91	0.0675	63.45	33.22	100.00	1.00
50-75% (NH4)2SO4	25	1.25	2.2094	55.24	44.19	87.05	1.33
DEAE-cellulose (P1)	2.5	0.163	2.1483	5.37	32.95	19.71	1.82
DEAE-cellulose (P2)	4.7	0.255	1.5191	7.14	28.00		
Sephacryl S-200(P1)	2.7	0.066	1.8477	4.99	75.59	15.22	3.18
Sephacryl S-200(P2)	2.4	0.162	2.0242	4.86	29.99		

Biochemical Properties of Proteases

The effect of pH on casein hydrolytic activity was assayed in 50 mM NaOAc-AcOH (pH 4-5.5), 50 mM MES-NaOH (pH 6-7) and 50 mM Tris-HCl containing 100 mM NaCl (pH 7.5-10). Enzyme activity was detectable over a neural range, from pH 6 to 8, as shown in Fig. 2. The activities in 50 mM MES-NaOH (pH 6-7) are overall lower compared to the neutral buffer, probably because of the specific buffer effect on the enzyme activity. The maximal enzyme activity in Tris-HCl buffer was obtained at pH 7.5-8.0. To estimate the optimal temperature, the proteases were

Table 2. Inhibition of caseinolytic protease activity

Inhibitors and chemicals	Concentration	Remaining protease activity (%)		Protease type
		P1	P2	
EDTA	1 mM	10	29	Metallo
	0.1 mM	11	33	
EGTA	10 mM	9	3	Metallo
	1 mM	10	18	
	0.1 mM	9	39	
1,10-phenanthroline	10 mM	0	0	Metallo
	1 mM	3	0	
	0.1 mM	55	34	
Phosphoramidon	5 mM	2	45	Metallo
	0.5 mM	2	80	
	0.05 mM	12	87	
Galardin	50 ug/ml	0	71	Metallo
	5 ug/ml	12	104	
	0.5 ug/ml	37	103	
PMSF	1 mM	101	110	Serine
	0.1 mM	87	95	
SBTI	1 mg/ml	35	77	Serine
	0.1 mg/ml	65	144	
	0.01 mg/ml	83	136	
Leupeptin	10 mM	95	75	Serine
	1 mM	106	106	
	0.1 mM	106	111	
Suc-AAPV-CMK	1 mM	93	104	Elastase (serine)
	0.1 mM	94	108	
	0.01 mM	89	87	
Pepstatin A	5 mM	68	32	Acid (carboxylic)
	0.5 mM	75	86	
	0.05 mM	78	88	
E-64	5 mM	74	59	Thiol (cysteine)
	0.5 mM	76	78	
	0.05 mM	80	84	
SDS	1%	21	35	Surfactant
	0.10%	87	22	
	0.01%	243	132	
L-Cysteine.HCl	10 mM	0	0	Cysteine
	1 mM	108	100	
	0.1 mM	119	116	
β-mercaptoethanol	1 mM	133	106	Sulfohydryl
	0.1 mM	121	113	
DTT	10 mM	35	15	Sulfohydryl
	1 mM	84	65	
	0.1 mM	123	115	

assayed for casein hydrolytic activity at 21, 37, 50, and 70 °C. The optimal temperature was between 37 and 50 °C as shown in Fig. 3. The effect of various inhibitors and chemicals on protease activity is presented in Table 2. P1 was rapidly inhibited by metal-chelating agents such as EDTA, EGTA, 1,10-phenanthroline, phosphoramidon, and galardin. P2 was also rapidly inhibited by metal-chelating agents such as EDTA, EGTA, 1,10-phenanthroline, but was relatively less sensitive to phosphoramidon and galardin. Sulfhydryl reagent DTT, soybean trypsin inhibitor (SBTI), and SDS inhibited P1 and P2 activities with some variable extents as well. Of note, 0.01% SDS activated P1 activity approximately 2.4-fold relative to control, suggesting certain activation mechanism of the enzymatic activity. Divalent metal ions Cu^{2+}, Fe^{2+} and Zn^{2+} inhibited caseinolytic activities of P1 and P2, whereas Ca^{2+}, Mg^{2+} and Mn^{2+} did not (Table 3). Inhibition analysis with specific protease inhibitors and various divalent ions suggested that P1 belongs to family M4 Zn-metalloprotease, while P2 does not. Furthermore, P1 and P2 enzymes appear to require zinc for hydrolytic activity, since the addition of 1 mM 1,10-phenanthroline to the assay mixture completely abolished the activity against casein, even in the presence of excess $CaCl_2$ (1 mM). This is supported by identification of the enzymes, which have high homology with M4 and M6 Zn-metalloproteases for P1 and P2, respectively (see below).

Identification of proteases

To identify the proteases and to determine the cleavage site from preproenzyme, we sequenced the N-terminal amino acid by an automated microsequencing system. N-terminal sequence of P1 protease was determined to be KPVTGTNAVG as a major sequence and VTGTNAVG as a minor sequence, which is identified to be a thermolysin-like neutral protease (BA0599) (observed MW 36kDa; calculated MW 34.08 kDa), belonging to family M4. The data base search showed that the sequence is similar to lactobacillus hydrolase (BAA06144, 99.3% identity), *B. cereus* neutral protease (AAZ42070, 99.1% identity), bacillolysin (YP_034856, 97.7% identity) and bacillolysin MA (BAD60997, 72.3% identity), all of which belong to neutral protease family (Npr).

Table 3. Caseinolytic ctivity of proteases in the presence of divalent ions

Divalent ion	Concentration (mM)	Remaining activity (%)	
		P1	P2
Control		100	100
Ca2+	1	86	91
	0.1	97	94
Cu2+	1	0	0
	0.1	1	0
Fe2+	1	0	0
	0.1	63	48
Mg2+	1	83	76
	0.1	97	97
Mn2+	1	79	103
	0.1	96	91
Ni2+	1	46	45
	0.1	77	69
Zn2+	1	21	0
	0.1	78	51

The amino acids at putative signal peptide cleavage site, propeptide cleavage site, zinc binding site, and active site in protease P1 were highly homologous with those of Npr proteins. N-terminal sequence of P2 protease was determined to be TGPVRGGLNG for 46 kDa and SNGTEKKSHN for 18 kDa protein, which was identified to be immune inhibitor A metalloprotease (BA1295), belonging to family M6. This data indicates that the 18 kDa protein (calculated MW 18.1 kDa) is an auto-processed product of immune inhibitor A metalloprotease (InhA) like that of *B. cereus*. Unlike InhA of *B. cereus*, however, which was found in the exosporium as a loose-fitting, balloon-like layer enclosing the spore (Charlton *et al.,* 1999), the InhA of *B. anthracis* is secreted to the culture broth. This is consistent with analysis data of extracelluar proteomes of non-virulent *B. anthracis* UM23C1-2 (Antelmann *et al.*, 2005).

Table 4. Host protein cleavage by isolated proteases

Category	Protein	P1	P2
Extracellular matrix proteins	Type I	+	+
	Type IV	(+)	+
	Fibronectin	+	+
	Laminin	+	(+)
Immune related proteins	Immunoglobul	(+)	(+)
	Interferon	-	-
Tissue damage/ Hemorrhage	Plasminogen	(+)	+
	α1-Proteinase	+	+
	α2-	(+)	(+)
	Fibrinogen	+	+ (Aα,

Substrate Specificity:

We used the internally quenched fluorogenic substrates of casein, gelatin and elastin to investigate the substrate specificity of isolates enzymes. P1 has strong activity for casein (14.09 U/mg) and elastin (17.48 U/mg) and relatively weak activity for gelatin (6.47 U/mg). On the other hand, P2 has strong activity for casein (14.26 U/mg) and gelatin (16.28 U/mg) but relatively weak activity for elastin (4.25 U/mg). Since bacterial protease may cause tissue damage by directly degrading host tissues, we tested several significant host proteins for degradation by the isolated proteases. For example, extracellular matrix proteins such as fibronectin, laminin, type I and IV collagen are often degraded during inflammation and bacterial infection. The results are summarized in Table 4. Protease P1 cleaved fibronectin, laminin, type I collagen effectively, and type IV collagen to a lesser extent. Meanwhile, the protease P2 effectively cleaved fibronectin, type I and IV collagen, and laminin to a lesser extent. It is known that α_2-macroglobulin and α_1-protease inhibitor (antitrypsin) are the most important serum protease inhibitors regulating the activity of plasmin and blood elastase, respectively. We show that α_2-macroglobulin and α_1-protease inhibitor are effectively degraded by the *B. anthracis* proteases. Purified enzymes did not prominently digest immunoglobulin A (IgA) and interferon-γ. Only small cleavage peptides of IgA were formed,

as shown in Fig. 4. Fibrinogen chains of α- and β-type were completely cleaved by protease P1 after 4 hours of incubation unlike the γ-chains, which remained visible in the gel. On the other hand, all fibrinogen chains were cleaved completely by protease P2. In cleaving human plasminogen by protease P1 and P2, the latter is more active than P1. After incubation for 4 hours at 37 °C with 0.2 μg enzyme, plasminogen was cleaved into at least 5 fragments as seen in reduced SDS-PAGE, which are similar to cleavage of plasminogen by bacillolysin MA (Narasaki *et al.*, 2005). Taken together, these suggest that anthrax extracelluar proteases may cause direct tissue damage to the host or damage to host tissue through a modulation of the host's plasmin-mediated inflammation system. *Synd shedding by proteases*

It has been previously reported that some bacterial agents can cause enhanced host ectodomain shedding (ES) which contributes to epithelial barrier disruption, endothelial damage, and tissue penetration (Park *et al.*, 2000; Park *et al.*, 2001;Park *et al.*, 2004). Shed ectodomain can play signaling role as a mediator of lethality perturbing different mechanisms of the host defense response. Therefore, we studied whether anthrax extracellular proteases can modulate Synd shedding of host cells. Purified protease P1 and P2 enhanced Synd shedding of NMuMG (normal murine mammary gland epithelial) cells in a time-dependent and in a dose-dependent manner (Fig. 5). Notably, protease P2 showed stronger activity than P1. Cell lysis (as LDH release) was measured to check the cytotoxic activity of P1 and P2 proteases to NMuMG cells. As shown in Fig. 6, P1 is slightly cytotoxic to the cells in a concentration-dependent manner, whereas P2 is not cytotoxic even in a high concentration of 1 μg/ml.

Synds are a transmembrane heparan sulfate proteolgycans expressed on all adherent cells. Heparan sulfate attached to the Synd core protein is a ubiquitous glycosaminoglycan (GAG) and regulates a wide variety of biological processes including hemostasis, inflammation, angiogenesis, growth factors, cell adhesion, and many others. Literature data show that regulatory functions of GAGs can be achieved through the interaction with proteases. For instance, cathepsins inhibit collagenase activity by GAGs. Therefore, we investigated the interaction of heparin/heparan sulfate with the purified proteases and the effect of GAG on the enzyme activity. The interaction of the protease with heparin was observed by heparin-Sepharose affinity

chromatography in 50 mM sodium acetate buffer (pH 4.5). The P1 protease was eluted from heparin column at ionic strength of 0.15 M, suggesting a weak binding of the protease with heparin (Fig. 7a). Furthermore, P1 protease was inhibited by heparan sulfate in a concentration-dependent manner (Fig. 7b). These results suggest a regulatory or host defense mechanism underlying pathogenic protease and cell surface Synd. Future experiments will clarify if the proteases enhance Synd shedding by stimulating the host cell shedding mechanism or directly shed Synd from cell surface.

Molecular cloning of proteases

To confirm properties and biological activities of the purified enzyme and to raise antibodies against the proteins for neutralizing the activity, we attempted to make recombinant proteases for P1 (BA0599) and P2 (BA1295) metalloproteases. DNA fragments encoding mature proteases were amplified by PCR with a Platinum Taq DNA polymserase. The resulting products were cloned into pTrcHis2-TOPO expression system with a 6X His-tag at C-terminus. In the case of P2, two isoforms (full-length of mature form and C-terminal truncated mature form) were cloned. Expression of the cloned proteins was obtained from *E. coli* TOP10 cells after IPTG induction for 4.5 hours. Under native conditions, batch purification of recombinant proteins was performed. Following centrifugation of the lysates, the proteases were not found in the supernatant but were located in the pellets. Fractionation of *E. coli* cells demonstrated that the recombinant proteases are insoluble, which suggest that the recombinant proteins reside in inclusion bodies. Thus, cell lysates were prepared under denaturing conditions with 8 M urea. The recombinant proteins were eluted from a Ni-NTA column by pH change of buffer to 5.9. Fig. 8 showed the purification of the proteases by Ni-NTA chromatography. P1 showed a single polypeptide in SDS-PAGE as major protein but P2 showed two bands in each clone of full-length and C-terminal truncated isoform. Refolding for biological evaluation and boosting antibody of the recombinant proteases will be performed in the future experiments.

Anthrax infection in mice is accompanied by acceleration of soluble Synd1, Synd4 shedding

In order to prove our hypothesis that epithelial cell ectodomain damage takes place in anthrax we first tested if Synd shedding accompanies anthrax systemic infectious process in mice. Synds 1 and 4 are abundant on the epithelial cells and can be assayed using antibodies specific to the corresponding core proteins or the HS chains. The DBA/2 mice were challenged with *ca.* 30x LD_{50} of *B. anthracis* spores of the toxigenic Sterne strain intraperitoneally as described before (Popov *et al.*, 2005). Blood samples were drawn, and serum was blotted onto a nylon membrane in conditions when highly charged HS polymers are selectively retained by the membrane. Analysis of the dot-blot intensities after immunodetection shows a several-fold increase in the amount of shed Synd1 and Synd4 on the next day post challenge (Fig. 9). A high level of circulating ectodomain is sustained until two days post-infection. In the conditions of the experiment, animal death begins at day 3, and all animals die by day 6. The onset of death on day 3 is accompanied by a decrease in the dot blot intensity for both Synds, however the amount of HS detected with a specific antibody remains sturdily elevated. The observed effect can be explained by a number of alternative mechanisms, such as degradation of Synd core proteins resulting in the loss of their immunoreactivity with antibodies, or heparanase-mediated cleavage of Synd HS chains from the core protein, which could lead to a reduced retention of the protein on the assay membrane and consequent decrease in the immunoblot signal. In any case, the abnormal release of HS into circulation of infected mice directly indicates that the pathological acceleration of Synd shedding takes place *in vivo* at systemic level and is accompanied by the processes of its biochemical turnover (Yanagishita and Hascall, 1992).

LT and hemolytic factors increase ectodomain shedding from NMuMG cells

The above results on shedding in mice challenged with anthrax spores prompted us to study if known anthrax virulence factors can accelerate shedding in the *in vitro* system. We therefore performed experiments with the isolated recombinant proteins identified by us as candidate shedding inducers, namely LT and hemolysins AnlO, AnlB and ClnA using NMuMG epithelial cells.

This murine cell type represents a commonly used model in similar studies (Park *et al.*, 2004). We found that all tested hemolytic proteins, as well as LT cause a dose-dependent acceleration of Synd1 release into supernatants. The individual components of LT, the protective antigen (PA) and the lethal factor (LF) do not induce shedding (Fig. 10). This suggests that neither the extracellular enzymatic activity of LF nor the sole pore-forming capacity of PA is directly responsible for shedding. The time cause of Synd1 release in the case of AnlO shows that the amount of shed Synd increases 4-fold within 30 min and continues to grow for several hours albeit with a slower rate (Fig. 11). The LT causes statistically reliable increase in Synd1 shedding, although the effect of LT develops slower compared to AnlO (Fig. 11).

Analysis of cell viability in the shedding experiments reveals a marginal to small degree of LDH release from treated cells compared to untreated ones. There is no obvious correlation of cell death with the amount of shed Synd1, which allows us to conclude that the processes of shedding and cell death are not directly related to each other but rather take place concomitantly, depending on the nature of the pathogenic factor and other treatment conditions. For example, treatments with either ClnA or AnlB are not cytolytic while the amounts of shed Synd1 in both cases increase 8-fold. AnlO increases cell death 3–fold (from 2% to 6%), while there is an 11-fold increase in Synd1 shedding. In the case of LT, incubation for 24 h leads to a 1.6-fold increase in cell death (from 10% to 16%), while the amount of shed Synd1 increases almost 3-fold. This conclusion agrees with direct microscopic observation of treated monolayers displaying live cells with partially or completely shed Synd1 using fluorescently-labeled anti-Synd1 antibodies (see below). We did not explore this topic further, however available data show that apoptosis followed the E-cadherin shedding in enterocytes (Fouquet *et al.*, 2004), while in endothelial cells LT compromised the barrier integrity (presumably through ectodomain shedding) independently of apoptosis or necrosis (Warfel *et al.*, 2005). Stimulation with the phorbol ester, a known inducer of shedding (Fitzgerald *et al.*, 2000), prolonged viability of epithelial cells (Kirby, 2004) and predisposed monocytes to apoptotic death caused by LT (Kassam *et al.*, 2005).

In order to confirm the biochemical identity of shed Synd1, several control experiments have been carried out. Western blot of NMuMG cells supernatants after treatment with either LT,

ClnA, AlnB or AlnO using anti-mouse Synd1 antibody demonstrates an a high molecular mass smear band that can be attributed to the presence of heterogeneous heparan sulfate glucosaminodlycan chains in shed Synd1 (Fig. 12). Indeed, digestion of the supernatants with haparanase II and chondrotine sulfate ABC lyase leads to the appearance of a single band corresponding in gel mobility to the core Synd1 protein, which typically migrates in a gel as an approximately 80 KD band (Park *et al.*, 2004).

Immunostaining of the NMuMG monolayers with fluorescently-labeled antibodies against E-cadherin and Synd1

We examined the NMuMG cells grown on glass slides using immuno-fluorescence microscopy. After challenge with proteins causing Synd1 shedding the cells were fluorescently stained using E-cadherin- and Synd1-specific FITC-conjugated monoclonal antibodies. E-cadherin is a major transmembrane component of the apical junctional complex. In a simple polarized epithelium the later consists of tight junctions and underlying adherens junctions playing a key role in formation and maintenance of epithelial barriers (Ivanov *et al.*, 2005). We therefore wanted to see if the process of Synd ectodomain shedding observed in our experiments is accompanied by the loss of intercellular contacts reflected in the dissociation of the junctional complex. Our analyses revealed dramaticcytopathogenic changes in treated NMuMG cells. In all cases, a perfect network of E-cadherin visible in untreated confluent cells becomes disorganized, damaged and disappears from intercellular contacts upon treatment (Fig. 13). A partially confluent NMuMG cells demonstrate intensive Synd1 staining along the perimeter of cells, which partially or completely disappears from cell surfaces after incubation with the shedding-inducing proteins while remnants of the ectodomain remain visible in the intercellular space (Fig. 14). Notably, the treated cells retain a high intensity of DAPI blue fluorescence typical for undamaged nuclei, indicating that the loss of E-cadhering and Synd1 takes place from viable cells.

Inhibition of Synd1 release by anthrax LT and hemolytic factors

The ectodomain shedding of cell surface molecules is typically mediated by metalloproteinase sheddases (Fitzgerald *et al.*, 2000 ; Arribas and Borroto, 2002). Both constitutive and accelerated shedding are inhibited by a variety of substances active in a number of receptor- and stress-activated signaling pathways, which involve protein tyrosine kinases (PTKs), protein kinase C (PKC), and mitogen-activated protein kinases (MAPKs) (Fitzgerald *et al.*, 2000; Arribas and Borroto, 2002; Park *et al.*, 2004). The activity of LT in macrophages and epithelial cells has been previously reported to involve MAPK kinase cascades (Duesbery *et al.*,1998; Kirby, 2004).

The results of inhibition experiments are presented in the Table 5. Piceatannol, a specific inhibitor of the Syk family of PTKs (Wong and Leong, 2004) is active in both spontaneous and induced Synd1 shedding for all tested proteins. In the case of AnlO and LT at low concentration of 0.5 μM the inhibitor shows some stimulatory effect on both constitutive and induced shedding but it strongly inhibits Synd1 release in a typical for its activity range of 5 to 50 μM (Mahabeleshwar and Kundu, 2003). The effect of piceatannol suggests that all four factors stimulate signaling pathways, which most probably involve cytoplasmic Syk, however piceatannol has also been reported to inhibit other tyrosine kinases in a similar concentration range. In agreement with the above suggestion the inhibitor of Src PTK family PP2 is completely inactive (data not shown). A general PTK inhibitor tyrphostin A25 (at 0.5 to 5 μM) shows only a weak activity. The phosphatidylinositol-3-kinase inhibitor LY294002 is inactive with all tested proteins, and we conclude that the cell survival pathway mediated by this kinase is irrelevant to shedding.

Suramin is a multi-potent therapeutic (Ralevic and Burnstock, 1998), which among other activities displays an antitumoral effect by blocking the growth factor binding to several receptors, including the ones for epidermal growth factor (EGF), platelet derived growth factor (PGDF), insulin growth factor II, and transforming growth factor-β (TNF-β) (Botta *et al.,* 2000). These growth factors bind to heparan sulfate-containing proteoglycans, which can be shed in various patho-physiological processes, such as wound repair, and microbial infections (Kheradmand and Werb, 2002; Arribas and Borroto, 2002). Most importantly, suramin modulates activity of protein tyrosine phosphatases (PTPs) involved in cell adhesion, integrin signaling and cell cycle progression (Zhang *et al.*, 1998; Stoker, 2005). Among these, PTP1B and Cdc25A are inhibited by suramin in

the low μM range. The drug has low bioavailability, and requires concentrations of 50 μM and higher to activate PTPα and PTP LAR (MacCain *et al.*, 2004). Table 5 shows that similar to piceatannol, suramin stimulates shedding at 20 μM. At higher concentration, suramin effectively inhibits Synd1 shedding in NMuMGs induced by LT and AlnO. This effect is consistent with the inhibition-activation pattern of suramin activity toward PTPs but the multi-potency of suramin excludes its clear interpretation without additional studies. Shedding activities of lipases ClnA and AnlB are insensitive to suramin at all concentrations tested.

In order to understand which signaling pathways among p38, ERK and JNK are involved in LT-mediated acceleration of Synd shedding we tested SB202190, an inhibitor of p38; PD98059, an inhibitor of MEK1/2 (ERK pathway); and the JNK inhibitor II. While both AnlO and LT induce Synd1 shedding, LT on itself is a known inhibitor of MAPK signaling (Duesbery *et al.*, 1998). In contrast, AnlO was reported to stimulate p38 in macrophages (Park *et al.*, 2004). We found that the p38 inhibitor in the range of 1 to 10 μM decreased Synd1 shedding in NMuMGs induced by either AnlO or LT to the level of spontaneous shedding observed in cultures without treatment but it is inactive with ClnA and AnlB. The inhibitor of ERK pathways PD 98059 (at 5 to 50 μM) behaves similar to SB202190 with AnlO but it is less effective in the LT-induced shedding. The only detectable effect of the JNK inhibitor is the stimulation of shedding by sphingomyelinase AnlB. None of the tested inhibitors is toxic to cells in the conditions of the inhibitor experiments (viability of inhibitor-treated control cells remains at the level above 90%, data not shown) indicating that activity of tested inhibitors is not dependent on their cytotoxic effect. ERK1/2 and p38 phosphorylation patterns were studies in more detail. Fig. 15 shows that the AnlO-treated cells reveal a massive transient ERK1/2 activation lasting for more than 4h in the presence of 1 μg/ml AnlO. Less concentration of AnlO causes a shorter period of activation.

ERK1/2 and p38 phosphorylation patterns in NMuMGs treated with AnlO or LT

Since both PD98059 and SB202190 influence the AnlO- and LT-induced Synd1 shedding,

Table 5. Effect of inhibitors on Synd1 ectodomain shedding from NMuMG cells enhanced by *B. anthracis* proteins

Inhibitors	Shed Synd1 (mean % of no-inhibitor control ± C.I.)				
	Spontaneous	CnlA	AnlB	AnlO	LT
No inhibitor	100±11	100±9	100±12	100±22	100±1
Tyrphostin A25					
5 μM	86±6			73±23	97±8
50 μM	72±7	100±9	85±17	67±7	81±4
Piceatannol					
0.5 μM	191±31			136±30	199±15
5 μM	112±24			88±25	79±12
50 μM	46±4	17±9	6±2	14±9	25±2
Suramin					
20 μM	160±27			155±26	144±14
200 μM	36±4	89±17	118±7	25±4	34±4
PD98059					
5 μM	130±10			84±5	90±4
50 μM	133±4	103±15	88±3	56±5	77±4
SB202190					
5 μM	97±10			72±1	69±4
50 μM	91±10	108±17	101±19	39±1	37±5
JNK inhibitor II					
1.5 μM	125±9			89±5	109±7
15 μM	145±9	92±13	129±31	90±5	103±3

In both stimulated and unstimulated cells the ERK1/2 signal is followed by the increase in p38 phosphorylation. The LT also causes transient activation signals but its effect on the amounts of activated ERK1/2 and p38 is different from that of AnlO: the up-regulation of ERK1/2 phosphorylation is detectable at the 10 min time point and then it completely disappears within 30 min. While the transient peak of p38 activation is clearly detectable, its level remains lower compared to AnlO. It seems that the enzymatic cleavage of MAPKKs by LT is an important factor reducing the intensity of signaling, which ultimately drops below the level of untreated cells.

Collectively, the inhibition experiments demonstrate that *B. anthracis* pathogenic factors induce Synd1 shedding through different signaling pathways, which seem to converge on

activation of cytoplasmic PTKs. Among tested proteins, one can preliminary identify two groups of shedding inducers. The first one includes LT and pore-forming AnlO influencing MAPK pathways, which are commonly activated in response to receptor stimulation and stress, while the other consists of membranolytic lipases AnlA and AnlB.

Anthrax LT and hemolytic factors compromise epithelial barrier permeability

After our findings firmly established the fact of accelerated Synd shedding, it was important to test if the latter is accompanied by changes in barrier permeability. We used a primary culture of human small airway endothelial cells (HSAECs) grown on collagen-coated membranes with the pores permeable to Dextran Blue 2000, which was used as an indicator of barrier integrity (Sawai *et al.*, 2000). The membranes separated the lower and the upper chambers of the culture wells. The cells were challenged by adding AnlO, ClnA or LT in the upper chambers for 4 h. After treatment, Blue Dextran 2000 was added to the upper chambers for 2 h. The changes in barrier permeability were evaluated by measurements of optical absorbance of Blue Dextran 2000 in the lower chambers, in comparison with untreated cells. Fig. 16A shows that the AnlO and ClnA cause intensive shedding of Synd1. In these experimental conditions the LT challenge does not induce shedding (which becomes detectable only after the 24 h treatment; data not shown) and therefore serves as a negative control. In general, the HSAECs display the pattern of sensitivity to AnlO, ClnA and LT similar to that of the NMuMG cells. As expected, the acceleration of Synd shedding by AnlO and ClnA correlates with the increase in barrier permeability (Fig. 16B). This suggests a possible causal relationship between the two processes, which needs to be elaborated in further studies. Regarding the purpose of this report we conclude that the abnormal level of Synd1 shedding detected in the spore-challenged mice likely indicates the compromised epithelial barrier permeability induced by anthrax secreted factors at the early stages of the disease.

3. Task 3. Toll-Like Receptor (TLR)-Neutralizing Antibodies And Soluble TLRs As Specific And Broad-Spectrum Protection Against Biological Weapons

3.1. Background

The initial interaction of the bacterium with the host involves various aspects of innate immune response from epithelial cells, macrophages, neutrophils, and a host of other cells. TLRs have been shown to be an important part of the innate immune system in individual cells, responding to pathogen-associated molecular patterns (PAMPs) common to bacteria and viruses. Recent data demonstrate that functions of TLRs are considerably broader that sensing of PAMPs. A new paradigm of TLR-mediated activation implicates wounding and stress as important stimulants of inflammatory response, and therefore TLRs are likely to be activated upon significant cellular/tissue injury and damage. TLRs can serve as sensors of tissue well-being, and a variety of endogenous substances, including fibrinogen, fibronectin extra domain A, hyaluronic acid released from extracellular matrix, and perhaps heat shock proteins can trigger TLR-4 and thus might be considered potential mediators of the systemic inflammatory response (SIRS) (Johnson *et al.*, 2003). SIRS can be induced by the breakdown products of heparan sulfate proteoglycan. Rapid enzymatic degradation of heparan sulfate activates TLR-4, and when this activation reaches a threshold, the pathophysiology of the syndrome of sepsis and ensuing death can occur (Johnson *et al.*, 2004). The process of cell/tissue injury during *B. anthracis* infection is mediated by the secreted virulence factors, which include proteases, lipases, and toxins, such as lethal toxin (LT). Our discovery of *B. anthracis*-induced ectodomain shedding suggests that soluble ectodomain molecules released during the infectious process could initiate a cascade of TLR signaling as host response to damage inflicted by the microbe. This hypothesis establishes a close interconnection between Tasks 2 and 3, and provides additional rationale for investigation of the role(s) of TLRs in anthrax. In agreement with this hypothesis, it has also been reported that treatment of macrophages with AnlO activates TLR-4 (Park *et al.,* 2004b). Shedding induced by AnlO suggests a plausible mechanism of this activation.

We have focused on degraded heparan sulfate proteoglycan as a potential trigger of sepsis syndrome, because, among these substances, only heparan sulfate proteoglycan is degraded by host elastase. into a soluble form that might activate TLR-4. Both pancreatitis and systemic inflammation lead to release of elastase into the blood and tissues (Keim *et al.*, 1997; Kawabata *et al.*, 2002). In murine models, pancreatic and neutrophil elastase induce the systemic inflammatory effects and respiratory distress syndrome seen in acute pancreatitis (Jaffray *et al.*, 2000a,b). In rat models, elastase inhibitors reduce the severity of symptoms associated with acute pancreatitis (Song *et al.*, 1999; Yamano *et al.*, 1998). In humans, serum elastase is a prognostic indicator for the severity of multiple organ failure as a result of acute pancreatitis (Ikei *et al.*, 1998). *B. anthracis* sereted proteases display a high level of elastase-like activity, and blockage of elastase improves outcome of anthrax in our experiments (Popov *et al.*, 2005). However, the release of *B. anthracis* lytic factors may also result in degradation of extracellular heparan-sulfated proteoglycans other than Synds, which can potentially interact with TLR-4. The lack of TLR functions negatively affects humans, at least upon acute infection. However, in a systemic model of polymicrobial sepsis encompassing standardized influx of the gut flora into the peritoneal cavity, mice benefit from the lack of TLR functions (Weighardt *et al.*, 2002), which indicates TLR-dependent mediation of harmful effects in acute infection.

TLR-2 blockage upon antibiotic therapy may substantially contribute to prevention of an excessive host immune reaction upon sudden release of large amounts of microbial products from disintegrating microbial cells. It may have to be complemented by blockage of further surface receptors, for which TLR-4 is a prime candidate, in order to facilitate inhibition of cell activation. Conversely, failure of therapy to compensate for a decrease in biocidal immune cell activity upon TLR blockage by antibiotic treatment might compromise a beneficial outcome (Bochud and Calandra, 2003). Therefore, blockage of TLR pathological agonists, such as Synds, may represent a more suitable strategy.

While investigation of TLR signaling in cell culture provides useful mechanistic information, less is understood about organ-specific damage, innate response during anthrax pathogenesis, and the role of TLRs in the context of a whole organism. We therefore sought to complement our *in*

vitro studies with the investigation of genomic response during disease progression in mouse organs. We chose three organ systems, the lung, spleen, and liver to study, as each is important to disease outcome. The lung is the primary entry point and first line of defense from spores during inhalational disease. Its susceptibility likely determines the disease outcome if it fails to provide the appropriate physical and immunological barriers to the bacteria. The spleen contains machinery for removing old and damaged cells, and mounting an immune response to antigens within the blood. The liver is important in clearing the blood of bacteria, cell debris, and toxic substances. Liver histopathology has also been noted to be particularly dramatic during anthrax. The genomic data we collected are currently in the process of active validation and analysis.

3.2. Results

TLR signaling by B. anthracis pathogenic factors

We used HEK 293 cells transiently transfected with the TLR-2 expression construct and an NF-kB reporter plasmid in order to test if secreted factors of *B. anthracis* activate TLR-2 signaling. For the TLR-4 signaling the HEK 293 cells were stably transfected with the TLR-4/MD-2 expression construct. In each experiment the NF-kB reporter plasmid was transiently transfected into the TLR-4-expressing cells.

Upon direct treatment of transfected cells, the *B. anthracis* culture supernatant produces a detectable TLR2-related signal, compared with a culture media used as a control for a possible contamination with signaling substances (Fig. 17, 18). The intensity of signal correlates with proteolytic activity of culture supernatant tested in these experiments, because a heat-treated supernatant posess no enzymatic activity and is inactive in TLR signaling (Fig. 18). In addition, stimulation of cells in presence of protease inhibitor phenanthroline, which was previously shown by us as a potent inhibitor of the supernatant gelatinase activity, abrogates signaling (data not shown). One of the possible mechanisms of the culture supernantant activity could be a shedding of ectodomain from HEK cells with a concomitant generation of TLR2 agonist(s), such as Synd-1 or heparan sulfate. In support of this suggestion we demonstrate that the conditioned media

produced by NMuMG cell after exposure of these cells to AnlO or AnlB acquires a capacity to signal through TLR-2 (Fig. 19). Preliminary data (not shown) indicate that shed Synd-1 purified from the conditioned media acts as a TLR-2 but not TLR-4 agonist. In contrast to the TLR-2, our parallel experiments with the TLR-4-transformed cells identified a strong inhibition of TLR4 signal, when an inhibitor of endotoxin activity polymyxin was added to the cells (Fig. 20). This result suggests that TLR4 signaling experiments need to be performed in strictly controlled conditions ensuring the absence of LPS contamination. From this standpoint the TLR-2 signaling system is more robust, because TLR-2 does not respond to LPS however contamination with other unidentified proteins could still present a problem.

A biologically relevant scenario of TLR activation in anthrax infection is unknown, however one can suggest that activation of macrophages upon initial contact with spores represents an important component of innate response. We therefore tested if anthrax spores of the toxigenic Sterne strain are capable of inducing the TLR response. HEK 293 cells with transfected TLR2 construct were incubated with different amounts of Sterne spores in the presence and absence of antibiotics. When antibiotics were present, the germination of spores was prevented, and we expected that surface antigens of the spores would be recognized by the TLRs and induce signaling. Indeed, we found a strong concentration-dependent TLR-2 response in the presence of antibiotics (Fig. 21). Surprisingly, when the spores were incubated with cells in the absence of antibiotics, the TLR-2 signal was completely suppressed below the level detected in control cells.

Murine microarray studies

We had previously determined that a dose of 10^7 *Bacillus anthracis* Sterne spores/mouse yields an approximately 50% mortality in 3 days in 9/10 week-old DBA mice. Treatment intraperitoneally with ciprofloxacin at 50 mg/kg initiated at 2 or 3 days post infection is ineffective, indicating that in our model the day 3 post infection represents "a point of no return" at the late stage of disease. This is consistent with knowledge of anthrax pathogenesis in primates and humans, and shows the importance of studying disease progression over the course of the first days of infection, when therapeutic intervention could be initiated. Using our murine model, we

decided to follow the course of disease progression from the perspective of whole tissue genomic responses.

The generated initial data were subjected to appropriate quality control, hybridization image quality analyses, and initial bioinformatics processing. For lung, 14 chips were used in the analysis representing 4 replicates for day 1; 5 replicates for day 2; and 5 replicates for day 3. For the spleen, 11 chips were used representing 2 replicates for day 1; 5 replicates for day 2; and 4 replicates for day 3. For the liver, 8 chips were used representing 2 replicates for day 1; 2 replicates for day 2; and 4 replicates for day 4. Gene expression ratios for each organ were normalized using Loess. Density plots of lung and liver samples showed evident time-dependent trends, with the numbers of genes having ratios greater than or less than zero increasing with time (Fig. 22). Spleen samples did not show a similar time trend but instead showed a greater proportion of response during day 2 than on either day 1 or day 3. A covariance principle component analysis (PCA) was done using normalized ratios for all genes. PCA for all samples showed evident differences between day 1, 2 and 3 samples (Fig. 23). Realtime PCR of 10 selected genes from all samples yielded good agreement with microarray data (data not shown). The course of infection could be illustrated in the numbers of genes detected to be significantly (greater than 2-fold over control) up and down-regulated over the course of time (Fig. 24 and Table 6). In general, each organ also showed similar trends in data where the change in ratios of expression was considered statistically significant (p-value < 0.05, Fig. 25).

The most dramatic down-regulation could be observed in Day 3 of all organs, at the point closest to the death of the animals. Interestingly, the highest level of 2-fold or more down regulation is most readily apparent in the liver on Day 3, which is consistent with current knowledge of the extreme histopathology of the liver during late stage anthrax. The highest number of 2-fold or more up-regulation can be observed in the spleen on Day 2, which follows the expected response of the spleen during infection as it is exposed to a high number of antigenic and immune-mediating compounds over the first 48 hours of infection.

We were very interested over the course of this project to follow the levels of innate immune response, particularly the levels of TLR receptor expression. By examining their levels of organ-wide

Table 6. Total numbers of spleen genes detected, and over 2-fold up- or down-regulated during anthrax disease progression.

Lung	Total # of genes detected	Over 2-fold up regulation	Over 2-fold down regulation
Day 1	2198	53	3
Day 2	11825	107	15
Day 3	10624	81	51

Spleen	Total # of genes detected	Over 2-fold up regulation	Over 2-fold down regulation
Day 1	4280	37	0
Day 2	8251	388	1
Day 3	8504	144	42

Liver	Total # of genes detected	Over 2-fold up regulation	Over 2-fold down regulation
Day 1	4051	51	0
Day 2	3289	15	0
Day 3	9081	26	280

expression during the 3-day course of pathogenesis, we hoped to get an indicator as to how many were being bound and activated. Following this would give us an idea of their importance during anthrax, and help us to determine whether or not a strategy of soluble TLRs to help mitigate the septic shock associated with the host innate-immune response would be a viable strategy in improving disease outcome. Table 7 shows the levels of expression of the majority of known TLRs in the mouse.

Of these, TLR-2 is the most relevant to bacterial infections, while TLR-4 is also important in wound repair and response. Other TLRs may respond to host and disease-induced mediators. In general, no significant increases or reductions were seen in any of the TLRs where they were detected, with a few exceptions. One interesting exception was observed in TLR2 of the spleen on Day 3 of infection. This is indeed the most likely place to expect large-scale turnover of TLR-2, however our degree of confidence in the data as indicated by the t-test is low.

Table 7. Microarray data of lung TLR gene expression during anthrax pathogenesis.

Lung	Day 1	T-Test	Day 2	T-Test	Day 3	T-Test
TLR 1	**0.510275**	0.240449	**1.252478**	0.21982	**1.096789**	0.710807
TLR 2	**0.833201**	0.247131	**1.043412**	0.558786	**1.303009**	0.005775
TLR 3	N/D	-	**1.406191**	0.000307	N/D	-
TLR 4	N/D	-	**1.236556**	0.138953	**1.038**	0.022192
TLR 5	**0.602866**	0.214359	**1.083796**	0.349058	**0.804117**	0.106556
TLR 6	**0.873866**	0.210447	**0.95438**	0.926659	**0.653333**	0.258865
TLR 9	**0.707778**	0.434257	**1.048672**	0.440505	**1.216203**	0.010934

Spleen	Day 1	T-Test	Day 2	T-Test	Day 3	T-Test
TLR 1	N/D	-	**1.004049**	0.53664	**1.008706**	0.710846
TLR 2	**0.956516**	0.553558	**0.962547**	0.309714	**1.828869**	0.725502
TLR 3	**0.957486**	0.047917	N/D	-	**1.064759**	0.80247
TLR 4	N/D	-	**1.124396**	0.033184	N/D	-
TLR 5	N/D	-	**1.010536**	0.070047	**1.00664**	0.977358
TLR 6	N/D	-	**0.945854**	0.454385	N/D	-
TLR 9	N/D	-	**0.849898**	0.289158	**1.20329**	0.117607

Liver	Day 1	T-Test	Day 2	T-Test	Day 3	T-Test
TLR 1	**0.862487**	0.890921	N/D	-	**1.253707**	0.001421
TLR 2	**0.866995**	0.553336	**1.072487**	0.353894	**1.148028**	0.069267
TLR 3	**1.113452**	0.915997	N/D	-	**1.215667**	0.001621
TLR 4	N/D	-	N/D	-	N/D	-
TLR 5	**0.859592**	0.811543	**0.912459**	0.417135	**1.062942**	0.125727
TLR 6	**0.790307**	0.766832	**0.943129**	0.737318	N/D	-
TLR 9	**0.948807**	0.335508	N/D	-	**1.024043**	0.193562

Normalized expression in the reference sample is 1. N/D signifies 'not detected.

Table 8. Microarray data of GTP-rho binding protein expression during anthrax pathogenesis

GTP-rho binding protein	Day 1	T-test	Day 2	T-Test	Day 3	T-Test
Liver	**1.838481**	0.338435	**2.24698**	0.033246	**1.512948**	0.009762
Spleen	**2.356543**	0.059817	**2.903556**	0.00133	**1.202411**	0.00133
Lung	**1.878458**	0.037511	**2.527159**	0.001271	**1.652112**	0.019196

Another indicator of the level of innate response is genes whose protein products are involved in the initial signal transduction cascade just inside the cell membrane. Several of these genes are indeed observed to be highly activated with a high degree of confidence, particularly those associated with G-protein signaling (Table 8).

This supports a hypothesis that despite an obvious turnover in TLR receptors, signal transduction and response systems are indeed being initiated. Since it is well-known that LT targets signals transduction pathways at the level of mitogen-activated kinases, we were interested in examining their level of turnover as well. Upstream of the primary MAPK kinase targets for LT, expression of MAPK kinase kinases (MAP3Ks) were followed (Table 9). It is interesting to note the high level of MAP3K12 upregulation, although confidence was low by t-test. MAP3K12 has been shown to be an important inducer of JNK/SAPK when overexpressed (Hirai *et al.,* 1996). A high degree of confidence was observed in the level of MAP3K8 downregulation. MAP3K8 has been shown to be an important negative regulator of Th1-type adaptive immunity, also inhibiting IL-12 production from accessory cells (Sugimoto *et al.*, 2004). Its downregulation is indicative of the bridge and transition between innate and adaptive immunity.

Downstream of MAP3Ks, at the level of MAPK kinases (MAP2Ks), slightly increased expression over the control is observed in most of the MAP2Ks implicated as targets for LeTx-induced enzymatic cleavage (Table 10). Interestingly, MAP2K5, which does not contain an enzymatic cleavage site and is not thought to be a target of LT is significantly down-regulated in all organs. So not only does this appear to support the current model of innate immune suppression, but it also hints at another pathogenic consequence of disease, which somehow brings about the down regulation of MAP2K5 without having to employ the enzymatic cleavage of its protein product. Our lab is particularly interested in host shedding of extra-cellular mediators as a consequence and pathogenic factor of anthrax. Shedding of proteoglycans such as Synd has been shown to induce pathogenic effects upon the host and activate innate immune responses. It was interesting that in this system, no significant increase in Syndecan expression was observed during the course of disease (Table 11) however Synd3 expression was significantly suppressed in the lung and spleen with a high degree of confidence.

Table 9. Microarray data of MAP3K gene expression during anthrax pathogenesis.

Lung

MAP3K	Day 1	T-test	Day 2	T-test	Day 3	T-test
Map3k1	**0.837757**	0.662397	**1.090654**	0.652392	**0.937669**	0.869405
Map3k2	**0.833134**	0.724808	**0.972461**	0.052322	**1.104085**	0.630675
Map3k3	N/D	-	**1.390267**	0.004567	**1.228146**	0.012615
Map3k4	N/D	-	**1.221793**	0.171539	**1.066536**	0.254849
Map3k5	N/D	-	**1.25417**	0.000935	**1.072504**	0.082238
Map3k6	N/D	-	**1.284782**	0.015468	**1.259227**	0.007436
Map3k7	N/D	-	N/D	-	**1.191147**	0.077567
Map3k8	**1.155022**	0.043981	**0.365778**	0.000946	**0.341165**	0.014261
Map3k11	N/D	-	**1.269466**	0.004051	**1.130793**	0.005109
Map3k12	**1.498149**	0.352564	**2.803323**	0.414263	**2.389418**	0.606283

Spleen

MAP3K	Day 1	T-test	Day 2	T-test	Day 3	T-test
Map3k1	**0.986917**	0.09356	**0.955837**	0.354994	N/D	-
Map3k2	**1.113135**	0.05231	**0.986987**	0.045237	**1.168807**	0.045237
Map3k3	N/D	-	**0.971121**	0.154599	**1.482875**	0.154599
Map3k4	N/D	-	**1.070928**	0.021306	N/D	-
Map3k5	N/D	-	**0.978337**	0.617281	**1.121732**	0.617281
Map3k6	N/D	-	**0.965196**	0.128138	**1.208133**	0.128138
Map3k7	N/D	-	**0.93066**	0.067043	N/D	-
Map3k8	**1.062614**	0.00744	**1.185148**	0.008533	**0.503525**	0.008533
Map3k11	N/D	-	N/D	-	N/D	-
Map3k12	**1.78799**	0.751423	**1.964004**	0.061671	**1.453909**	0.061671

Liver

MAP3K	Day 1	T-Test	Day 2	T-test	Day 3	T-Test
Map3k1	N/A	-	**1.035418**	0.827384	**1.072607**	0.81154
Map3k2	N/A	-	**0.956383**	0.710429	**1.124997**	0.025368
Map3k3	**0.930041**	0.450418	**1.15081**	0.087686	**1.219574**	0.002574
Map3k4	N/A	-	N/A	-	**1.135702**	0.103434
Map3k5	**0.968331**	0.481725	N/A	-	**1.345943**	0.004901
Map3k6	**0.985698**	0.464289	N/A	-	**1.255389**	0.00267
Map3k7	N/A	-	N/A	-	**1.130996**	0.086645
Map3k8	**1.228605**	0.22195	**0.637026**	0.034346	**0.326635**	0.035066
Map3k11	N/A	-	N/A	-	**1.064891**	0.217501
Map3k12	**1.905962**	0.085276	**1.334878**	0.292589	**1.302811**	0.763363

Normalized expression in the reference sample is 1. N/D signifies 'not detected'

Table 10. Microarray data of lung MAP2K gene expression during anthrax pathogenesis.

Lung

MAPKK	Day 1	T-test	Day 2	T-test	Day 3	T-test
Map2k1	N/D	-	**1.25477**	0.104129	**1.349424**	0.008655
Map2k2	N/D	-	**1.207824**	0.205538	**1.228208**	0.010077
Map2k3	N/D	-	**1.368791**	0.077504	**1.247078**	0.005089
Map2k4	N/D	-	**1.141449**	0.117334	**1.000375**	0.722445
Map2k5	**0.78834**	0.694314	**0.678633**	0.002122	**0.85001**	0.16217
Map2k6	**0.857387**	0.591962	**1.077345**	0.894299	**1.17321**	0.066626
Map2k7	N/D	-	**1.895034**	0.378901	**0.921345**	0.706903

Spleen

MAPKK	Day 1	T-Test	Day 2	T-test	Day 3	T-Test
Map2k1	N/D	-	**0.994605**	0.081658	**1.1391**	0.081658
Map2k2	N/D	-	**1.011425**	0.054454	**1.191836**	0.054454
Map2k3	N/D	-	**1.122482**	0.029519	**1.204075**	0.029519
Map2k4	N/D	-	N/D	-	N/D	-
Map2k5	**0.687183**	0.195005	**0.846139**	0.02227	**0.740337**	0.02227
Map2k6	**0.90876**	0.516853	**0.933954**	0.520025	**1.090801**	0.520025
Map2k7	N/D	-	**0.944365**	0.558869	**0.812283**	0.558869

Liver

MAPKK	Day 1	T-test	Day 2	T-Test	Day 3	T-Test
Map2k1	N/D	-	N/D	-	**1.112959**	0.008296
Map2k2	N/D	-	N/D	-	**1.322409**	0.066463
Map2k3	**0.922416**	**0.201649**	N/D	-	N/D	-
Map2k4	N/D	-	**0.922833**	0.386374	**1.051015**	0.255922
Map2k5	**0.985149**	**0.398778**	**0.807592**	0.292518	**0.743013**	0.104283
Map2k6	N/D	-	N/D	-	**1.131148**	0.098121
Map2k7	N/D	-	**1.055963**	0.231959	N/D	-

Normalized expression in the reference sample is 1. N/D signifies 'not detected'.

Table 11. Microarray data of syndecan and syndecan binding protein gene expression during anthrax pathogenesis.

Lung	Day 1	T-test	Day 2	T-Test	Day 3	T-Test
Syndecan 1	N/D	-	**1.202955**	0.120551	**0.951014**	0.109637
Syndecan 2	N/D	-	**1.126396**	0.73363	**1.296866**	0.005211
Syndecan 3	**1.07059**	0.03096	**0.561481**	0.000746	**0.678997**	0.157851
Syndecan 4	N/D	-	**1.196396**	0.437905	**1.007799**	0.077581
Syn Bind Prot	**0.803504**	0.47544	**0.993547**	0.52287	**1.161162**	0.309596

Spleen	Day 1	T-test	Day 2	T-Test	Day 3	T-Test
Syndecan 1	N/D	-	**0.971182**	0.230021	N/D	-
Syndecan 2	N/D	-	**0.986381**	0.282134	**0.942079**	0.282134
Syndecan 3	**0.720383**	0.014638	**1.010462**	0.046733	**0.569621**	0.046733
Syndecan 4	N/D	-	**0.979829**	0.595003	**1.032732**	0.595003
Syn Bind Prot	**0.888678**	0.276865	**1.070941**	0.532088	**0.854822**	0.532088

Liver	Day 1	T-test	Day 2	T-Test	Day 3	T-Test
Syndecan 1	N/D	-	N/D	-	**1.057366**	0.208784
Syndecan 2	**0.836906**	0.070676	**1.067368**	0.11839	**1.154518**	0.812139
Syndecan 3	**0.94653**	0.476282	**0.954672**	0.038625	**0.974245**	0.628491
Syndecan 4	**0.939342**	0.666363	N/D	-	**1.13198**	0.035096
Syn Bind Prot	**0.985125**	0.897135	N/D	-	**1.116765**	0.418193

Normalized expression in the reference sample is 1. N/D signifies 'not detected'

Discussion

This study reports isolation, purification and characterization of proteases from culture supernatants of *B. anthracis* ΔAmes strain (pOX1$^-$, pOX2$^-$) as an effort to elucidate the role of secreted proteases as candidate virulence factors. The proteases were purified from the crude culture supernatants using ammonium sulfate precipitation, DEAE-cellulose column chromatography, and an HPLC-aided Sephacryl S-200 gel filtration chromatography. In the DEAE-cellulose column chromatography, two major proteases were fractionated: one (P1) in a flowthrough, the other (P2) in 200 mM NaCl eluate. The purified enzymes showed a single protein band for P1 with a molecular weight of ~36 kDa and two bands for P2 with molecular weight of ~46 and ~18 kDa on reduced SDS-PAGE gel.

Sequence analysis by the automated Edman degradation of the proteins suggested that P1 protease belongs to the metalloprotease clan MA, family M4 (i.e., the thermolysin-like metalloproteases) and P2 belongs to clan MA, family M6 (i.e., immune inhibitor A metalloproteases). This is in agreement with our previous study (Popov *et al.*, 2005), which identified M4 proteases as new virulence factors in anthrax. In current report, we extended our analyses to M6 proteases. Although both P1 and P2 activity were inhibited by EDTA and 1,10-phenanthroline, P2 is not potently inhibited by phoshoramidon, a specific thermolysin inhibitor. Therefore, the inhibitor specificity of P1 is consistent with its similarity to thermolysin.

Bacterial proteases may cause tissue damage by directly degrading host tissues. In this study both P1 and P2 proteases were found to cleave the tissue components fibronectin, laminin, type I and type IV collagen with differential affinity. These data support our hypotheis that proteolytic degradation of extracellular matrix proteins in anthrax may play an important role in hemorrhage and bacterial invasion through endothelial and epithelial barriers (Popov *et al.,* 2005). Another important role of bacterial proteases in host-derived damage to tissues may consist in causing imbalance between neutrophil elastase and the host protease inhibitors, α_1-protease inhibitor and α_2-macroglobulin (Barbey-Morel and Perlmutter, 1991;Khan *et al.*, 1995) In agreement with this, we demonstrate that the proteases P1 and P2 from *B. anthracis* specifically cleave α_1-protease inhibitor (a neutrophil elastase inhibitor) and α_2-macroglobulin (broad-spectrum protease inhibitor). In addition to this, fibrinogen and plasminogen are degraded by proteases P1 and P2. Whether this cleavage by the proteases converts plasminogen to active plasmin is yet to be determined. According to similar cleavage pattern of plasminogen by the purified proteases such as bacillolysin MA, we believe the P1 and P2 employ host plasmin for bacterial invasion into host tissue, in addition to its own fibrolytic action. Thus, P1 and P2 protease from *B. anthracis* may contribute to anthrax pathology through direct degradation of host tissues (e.g., collagen, fibronection, laminin) and/or through modulation of host defenses (e.g., α_1-protease inhibitor, α_2-macroglobulin, plasmin).

Additional biological relevance of the purified proteases during *B. anthracis* infection can be found in their Synd shedding activity. Acceleration of ectodomain shedding represents a part of an adaptive response of the host cells to different stress factors and injury such as G protein-coupled receptor agonists, growth factors, cytokines, osmotic stress, wounding and phorbol ester (Li and Chaikof, 2002; Higashiyama Nanba, 2005; Hammermann and Hogger, 2005). However the functional significance of the ectodomain shedding in microbial pathology is uncertain: it could either promote pathogenesis or cellular defenses or both. Microbial membrane-damaging factors and other toxins can disturb cell homeostasis and serve as strong inducers of stress proceeding through activation of signaling pathways ultimately resulting in cytoskeletal rearrangements and increase in barrier permeability (Aktories and Barbieri, 2005). Although the cytoskeletal rearrangements and Synd1 ectodomain shedding are closely interconnected (Kato *et al.*, 1995; Beauvais and Rapraeger, 2004), a direct link between stress response, Synd1 ectodomain shedding and barrier dysfunction has never been demonstrated for bacterial toxins.

Initial evidence that *B. anthracis* toxins can disrupt host epithelial and endothelial barriers is available from early anthrax publications. For example, Smith *et al.* (1955) using LT produced *in vivo* identified vascular damage and renal failure as a consequence of its activity, while Smith and Stoner (1967) demonstrated that LT induced an increase in vascular permeability. These observations agree with the fact that the most damaged organs in the infectious process are the ones with high epithelial and endothelial cell content such as spleen, lungs, liver, renal system, vasculature of blood and lymphatic vessels. Recent report by Warfel *et al.* (2005) confirmed that LT can increase the endothelial barrier dysfunction independent of necrosis or apoptosis. The LT preparations used in early studies were crude, so we took into account a possibility that pathogenic factors other than LT could have played role in the observed effects. A spectrum of these factors includes (but may not be limited to) cytolytic lipases and pore-forming toxins (Mikshis *et al.*, 1999; Klichko *et al.*, 2003), and proteases of different specificity (Read *et al.*, 2003; Popov *et al.*, 2005).

Our data showed Synd1 shedding by protease P1 and P2 in NMuMG (normal murine mammary gland epithelial) cells in a time-dependent and in a dose-dependent manner without significant cytotoxicity. We will further explore this phenomenon based on our hypothesis that

release of soluble Synd1 and other ectodomain molecules could play a pivotal role in the inhalation anthrax pathology. Whether the proteases enhance Synd shedding by stimulating the shedding mechanism of the host cells or directly shed the Synd by proteolytic cleavage is yet to be examined by using experiments including application of inhibitors specific for Synd shedding and degradation of bacterial expressed Synd by proteases.

Our experiments demonstrate that in addition to proteases the bacterial secreted factors, such as pore-forming toxin AnlO, and cytolytic lipases ClnA and AnlB accelerate the normal process of host cell Synd and E-cadherin ectodomain shedding, which is as a proteolytic mechanism of releasing them in a soluble form (Hooper and Turner, 1999). We suggest that in anthrax this process can reach a pathological level compromising the epithelial integrity, and the full spectrum of proteins shed in anthrax requires further studies. Biologically relevant concentrations of anthrax shedding inducers in tissues, organs and body fluids are unknown, and therefore the assessment of each protein's contribution to ectodomain shedding *in vivo* is currently impossible, but the capacity of *B. anthracis* to produce hemolytic proteins, in addition to LT, has been demonstrated in both aerobic and anaerobic culture conditions (Mikshis *et al.*, 1999; Klichko *et al.*, 2003; Shannon *et al.*, 2003). The antibodies against these proteins are also detectable in serum of mice challenged with *B. anthracis* (Sterne) spores (data not shown). In our experimental conditions the release of Synd1 and E-cadherin takes place within several hours, and high levels of shed Synds are detectable after 24 hours post infection with spores (we have not tested earlier time points). This observation opens a possibility of using shed ectodomain release into circulation for early detection of the anthrax infectious process.

Normally, ES is mediated by metalloproteinases, which are collectively called sheddases or secretases. Our data agree with the host sheddase modulation mechanism demonstrated by others (Fitzgerald *et al.*, 2000; Park *et al.*, 2004; Higashiyama and Nanba, 2005), because metalloproteinase inhibitors such as galardin and phosphoramidon reduce shedding induced by AnlO (data not shown), which has no enzymatic activity on its own. Other anthrax proteins, ClnA and AnlB are not proteases, and therefore cannot shed Synd1 by direct proteolysis on the cell

surface. The LT is a metalloprotease but induction of Synd1 shedding requires LT delivery into the host cell, in agreement with the extracellular cleavage of the Synd1 core protein by cellular sheddase. The fact that proteins of absolutely different nature, such as proteases and lipases of distinct enzymatic specificities along with pore-forming toxins possessing no catalytic activity display similar effects with regard to Synd1 shedding indicates activation of a common intracellular mechanism by diverse extracellular signals. Indeed, the activity of piceatannol against shedding by all tested inducers suggests that cytoplasmic Syk PTK serves as the common point of convergence. This mechanism however retains a certain level of specificity judging by the fact that neither PA no LF induce shedding.

The MAPK-mediated pathways have been previously implicated in receptor-induced ectodomain shedding (Fitzgerald *et al.*, 2000). It has also been demonstrated that AnlO inhibited the p38 signaling in macrophages (Park *et al.*, 2004). Currently available data suggest that the p38 pathway defends against bacterial pore-forming toxins *in vivo* and *in vitro* (Huffman *et al.*, 2004) however we cannot conclude which of the MAPK pathways plays a predominant role in shedding. Both inhibitors of ERK1/2 (PD98059) or p38 (SB202190) decrease the AnlO-induced shedding. This effect agrees with the mechanism recently discovered for the hydrogen peroxide-stimulated cytoskeletal reorganization in endothelial cells (Nguyen *et al.*, 2004). It has been shown that both of the above inhibitors attenuated MAPK-mediated activation of the small heat shock protein Hsp27 downstream from ERK1/2 and p38. This protein is responsible for the actin stress fiber polymerization, which accompanies Synd ectodomain shedding (Kato *et al.*, 1995; An *et al.*, 2004; McMullen *et al.*, 2005). Kevil *et al.* (2001) reported that p38 inhibitor attenuated the oxidant stress fiber formation and prevented generation of gaps between endothelial cells. The LT shedding activity is also sensitive to MAPK inhibitors, however phosphorylation of both ERK1/2 and p38 is quickly suppressed before LT-induced shedding becomes readily detectable. Similar observation regarding the disruption of endothelial barrier permeability by LT allowed Warfel *et al.* (2005) to conclude that this effect of LT is somewhat paradoxical given that LT has been shown to inhibit MAPK signaling. We suggest that LT plays a dual role upon interaction with the host cells by inducing both the cellular stress and the inhibition of MAPK activation. The intricate combination of

both processes results in the reduction of the transient stress signal, which however remains sufficient for the induction of shedding but reduces the potency of LT as shedding inducer. In support of this, our data show that LT activity leads to a small but detectable activation of p38 even at high LT concentration. In contrast to LT the pretreatment of cells with the effective p38 inhibitor is expected to completely block the stress signal. This allows explain why chemical inhibition of p38 reduces shedding in our experiments and even increases the endothelial barrier resistance in the experiments of Warfel *et al.* (2005). Another precedent for this type of transient LT-induced MAPK activation effect has recently been described as toxin-induced toxin resistance in macrophages (Salles *et al.,* 2003).

The pathological significance Synd shedding in the anthrax infectious process needs to be further addressed in animal experiments. Our findings provide additional insights into the studies of anthrax virulence factors, such as LT, at cellular and organism levels, where shedding has to be taken into account as a mechanism, which could rapidly change epithelial and vascular permeability by the concerted effect of several pathogenic factors contributing to dissemination of infection, hemorrhages and edema. The shed soluble proteoglycans are highly-hydrated and this effect is expected to contribute to edema by causing influx of water into the intercellular space. Finally, shedding generates biologically active ectodomains that can function as paracrine or autocrine effectors (Bernfield *et al.*, 1999). It has already been shown that shed Synd1 is toxic to mice (Johnson *et al.*, 2001), and that inoculation of Synd1 ectodomain restored sensitivity of $Synd^{-/-}$ mice to *P.aeruginosa* (Park *et al.*, 2001). We suggest that induction Synd shedding by hemolysins and LT could substantially contribute to the development of anthrax septic shock.

A mechanism of anthrax septic shock is unknown. It could potentially involve activation of TLRs by shed ectodomain as a response to cell and tissue damage. This is in line with our original thought to develop soluble TLRs as a broad-spectrum treatment to help neutralize free antigens/mediators and inhibit the activation of cellular TLRs, thus helping to decrease the effects of the septic shock thought to occur near the end of disease progression. Indeed, several anthrax proteins, along with culture supernatant produced by the plasmid-negative delta Ames strain induce TLR2 activation. However, TLR2 signaling in HEK 293 cells in the presence of anthrax

Sterne spores is strongly inhibited. This observation is important, because it indicates an immunosuppressive effect of secreted factors produced by germinating Sterne spores. Therefore, we suggest that factors encoded by the pXO1 plasmid (such as lethal and edema toxins) could be responsible for the abrogation of the TLR signaling. This hypothesis will be tested in our future experiments however irrespective of the particular nature of the immunosuppressive substance produced by the germinating spores and vegetative cells, we anticipate that TLR stimulation seen in the experiments with individual proteins may not be biologically relevant to the infectious process. It is also apparent from our gene expression data that the TLR genes are not upregulated in all tested organs, and therefore mitigating the initial response induced by TLRs might not be as important for combating late stage disease as we originally proposed. Nevertheless, little is known about the actual level of TLR proteins on the surface after they are bound and activate their signal cascades, so the apparent lack of upregulation of TLR expression in our data does not necessarily indicate their lack of activation during infection.

In summary, our data suggest a possible connection between shedding and activation of TLR signaling in anthrax infection. We also show that individual pathogenic proteins and culture supernatants from the atoxigenic strain can cause activation of TLR-2 signaling however the factors produced by germinating spores and vegetative cells of the toxigenic strain effectively suppress the TLR-2 response. Therefore, it seems appropriate to further investigate if TLR activation in anthrax takes place. From this point of view, it is interesting to test if TLR2-neutralizing antibodies, such as recently described for TLR2-driven toxemia (Meng *et al.*, 2004) could be therapeutically useful for anthrax treatment. Meanwhile, the *in vitro* evidence needs to be obtained to support animal experimentation.

Materials and Methods

Protease Purification

Delta Ames strain ($pOX1^-$, $pOX2^-$) was cultured in a rich LB medium at 37 °C with vigorous agitation until the cells had reached stationary phase. The cells were removed by centrifugation at

17,000xg for 10 min. The culture supernatant of 940 ml was filtered to clear the cells out. The cell-free supernatant was precipitated with 50%- and 75%- saturation of ammonium sulphate. The precipitates were collected by centrifugation at 17,000xg for 20 min, and dissolved and dialyzed in 50 mM Tris-HCl (pH 7.6) containing 3 mM sodium azide. The precipitates by 75% saturation with ammonium sulphate were loaded onto a DEAE-cellulose anion exchange column (bed volume = 60 ml) equilibrated with 50 mM Tris-HCl (pH 7.6) containing 3 mM sodium azide. Elution was achieved step-wisely with concentration of 10, 50, 100, 200, 500, and 1,000 mM NaCl in the same buffer. The proteins were monitored at 280 nm and assayed for protease activity using EnzChek protease assay kits for caseinolytic, gelatinolytic and elastinolytic activity. Using the DEAE-cellulose column chromatography, two different proteases were fractionated: one (P1) in a flow-through, the other (P2) was eluted in 200 mM NaCl eluate. The P1 and P2 protease factions were subjected to a Sephacryl S-200 gel filtration column chromatography aided by HLPC.

Inhibiitors, reagents and isolated proteins.

NMuMG epithelial cells (CRL-1636) were from ATCC (Manassas, VA), human lung epithelial cells (HSAEC) were from Cambrex, Inc. (Walkersville, MD). DMEM media was from ATCC (Manassas, VA), other cell culture reagents were from Cellgro (Herndon, VA). Galardin, tyrphostin A25, piceatannol, suramin, SB202190, PD98059, JNK inhibitor II and PP2 were from Calbiochem (Darmstadt, Germany). Anti-human Synd1 antibody clone Mi15, rat anti-mouse Synd1 (clone 281-2), and rat anti-mouse Synd4 antibody KY/8.2 were from BD Biosciences (San Diego, CA). Anti-heparin/heparan sulfate antibody MAB-2040 was from Chemicon (Temecula, CA). Antibody against total and double phosphorylated p38 (Thr180/Tyr182), ERK (Thr202/Tyr204) and JNK(Thr183/Tyr185) were from Cell Signaling Technology (Beverly, MA). Hemolytic *B. anthracis* proteins were expressed in *E. coli*, purified and characterized as described before [13]. They are at least 95% homogeneous based on the results of SDS-PAGE analyses. The phospatidyl choline-preferring phospholipase C from *B. cereus* (cereolysin A) was purchased from Sigma (MA) and was used without further purification. Recombinant protective antigen (PA) and lethal factor (LF)

were purchased from List Biological Laboratories (Campbell, CA). The endotoxin content of all proteins was determined by E-toxate test (Sigma, MO).

Activation of shedding in cultured cells

Human Small Airway Epithelial Cells, or HSAECs (Cambrex, Inc., Walkersville, MD) were grown in DMEM/F12 complete medium with 10% fetal calf serum (FCS, Gibco). Before challenge the FCS content was reduced to 1%. NMuMG cells were grown up in Dulbecco's modified Eagle's medium with 4.5 g/l glucose, 10 µg/ml insulin, and 10% FCS. HSAECs were grown up in Ham's F12 media supplemented with non-essensial aminoacids, pyruvate, β-mercaptoethanol and 10% FCS. Cells were seeded in 96-well plates, cultured to 1 day post confluence, then stimulated with indicated proteins using serum-free media from Cellgro (Herndon ,VA) supplemented with 1% FCS. LT was used as a mixture of equal amounts of PA and LF at total concentration of 1.0 µg/ml, 0.1 µg/ml, and 0.01 µg/ml. After stimulation, the plates were spun down at 1,100 x g for 10 min and supernatant was frozen down at -20°C for further analyses. In control experiments, a known inducer of Synd1 shedding, PMA (4α-phorbol-12,13 didecanoate) in concentration 10 µM in 1% FCS media induced 4-fold increase in shed Synd-1 from NMuMG cells after 24 h incubation. In the same conditions, endotoxin in concentration 1 µg/ml did not induce significant shedding, and pre-treatment of AlnO (1 µg/ml) with polymyxin (50 µg/ml) had no effect on the amount of shed Synd1. Endotoxin contamination from added proteins in shedding experiments did not exceed 5 ng per ml of culture medium.

Dot Blot Assays

Supernatant from treated cells (100µl) was added to 1ml of acidification buffer (150mM NaCl, 50mM NaOAc, 0.1% Tween-20, pH 4.5). Immobilon NY+ membrane (9 x 12cm, Millipore) was prepared by first soaking it in acidification buffer. *Bio-Dot* microfiltration apparatus (Bio-Rad, CA) was used for all Synd dot blots. The sample wells were re-saturated with 100µl of acidification

to prevent drying of the membrane. 400µl of sample solution (in acidification buffer) was used per well on the apparatus. First the sample was kept in the wells on top of the membrane for 3 min and then it was drawn through the filter/membrane for another 3 min. The wells were rinsed twice with 400µl of acidification buffer. The membrane was taken out, rinsed twice for 5min in acidification buffer and blocked with 3% powdered milk in buffer #2 (150mM NaCl, 10mM Tris-HCl, pH 7.4) for 1 h. The membrane was then incubated with rat anti-mouse Synd1 antibody at a dilution of 1:1000 in 3% milk in buffer #3 (150mM NaCl, 10mM Tris-HCl, 0.3% Tween-20, pH 7.4) or mouse anti-heparan sulfate antibody for 2 h on a platform shaker at room temperature. For the cells of human origin the antibody against human Synd1 has been used in a dilution 1:2000. The membrane was then washed with buffer #3 three times for 5 min and incubated with goat anti-rat HRP-conjugated secondary antibody at a dilution of 1:7500 for murine Synd1 blot, or with goat anti-mouse HRP-conjugated polyclonal antibody at 1:1000 for the heparan sulfate or human Synd1 blots for 1 h at room temperature. The membranes were then washed again three times for 5 min with buffer #3. All membranes were developed using *ECL Plus* Western Blotting Detection kit (Amersham Biosciences, NJ) and Kodak BioMax Light Film (Sigma, MO). The results were quantified by scanning the exposed film, and evaluating the intensity of exposed dots by software AlphaEase FC (Alpha Innotech, San Leandro, CA). Results were expressed as amount of Synd shed in relative absorbance units (AU) using a calibration curve generated by two-fold dilutions of culture supernatants from *murine* or human epithelial cells treated with AlnO. The AUs varied between different experiments because of the exposition conditions and other treatment parameters. Each AU measurement represents the mean and the 95% confidence intervals calculated using the Student t-test.

Western blot of Synd1 after heparinase and chondroitinase digestion

Confluent NMuMG cells grown as described above were put in 1% FCS media with either ClnA, Aln B, Aln O or LT for 24h. After 24h, the floating cells were removed from supernatant by centrifugation, and proteoglycans in conditioned media were precipitated twice with 4 volumes of

95% ethanol containing 3% potassium acetate. Pellet was resuspended in 100 µM Tris-HCl, pH 8.0 containing 0.1 % Triton X-100, 5 µM EDTA, and 1mM phenylmethylsulfonyl fluoride. Half of each sample was incubated with both 10 mU/ml of heparan sulfate lyase and 25 mU/ml chondroitin sulfate lyase ABC (Seikagaku America Inc., Rockville, MD) for 5 h at 37°C. A fresh portion of enzymes was added after 2.5 h of incubation. Enzyme-treated samples (equivalent to 0.5 ml of conditioned media) were subjected to SDS-PAGE (3.5 to 20% gradient gel) and electro-transferred to Immobilon-N+ membranes (Bio-Rad, CA), which were processed as described above for the dot-blot immunoassay.

Synd-1 and E-cadherin immunostaining

NMuMG cells were grown to confluence on glass slides (BD Falcon and BD BioCoat) for 5 days and then challenged with indicated components. Cells were fixed for 10 min with methanol, washed 3 times with PBS, and then blocked for 20 min with 1% BSA in PBS. After washing with PBS, FITC-labeled murine monoclonal anti-mouse E-cadherin or anti-mouse Synd1 monoclonal antibodies (both from BD Transduction Laboratories) were used for 1 h staining in a dark, after which the slides were washed with PBS, mounted and examined under fluorescence microscope with appropriate filters. Vectashield mounting medium included diamidino phenyl indole (DAPI) for nuclear staining. According to the manufacturer, the anti-mouse E-cadherin antibody cross-reacts with human E-cadherin.

Analysis of mouse sera after challenge with B. anthracis spores

The 9 week old mice (DBA/2 from Taconic, Germantown, NY) were challenged intraperitoneally with $1x10^7$ spores of *B.anthracis* non-encapsulated Sterne strain 34F2 [$pXO1^+$, $pXO2^-$] obtained from the Colorado Serum Company (Boulder, CO). The 50% lethal dose of $3x10^6$ spores (LD_{50}) by the inraperitoneal (i.p.) route was established earlier [22]. Every 24 h interval post challenge, mice were anesthetized by intraperitoneal injection of Avertin (2,2,2 tribromethanol,

Aldrich), and were bled by cardiac puncture. Serum sample (20 µl) from each mouse was analyzed separately with dot blot as described above for cell culture supernatants.

Epithelial barrier permeability studies

HSAECs were grown on commercially available Costar inserts (Corning, NY) consisting of 12 mm permeable PTFE membranes with a pore size of 3.0 µm, and coated by the manufacturer with equal mixtures of Type I and Type III Collagen. Cells were seeded at concentrations of$1x10^5$ cell/ml and allowed to grow till confluency in DMEM/F12 complete medium with 10% FCS. Before challenge the FCS content was reduced to 1%. Epithelial barrier permeability to small molecules was evaluated after the cells were treated with shedding inducers by the addition of Blue Dextran 2000 (Sigma, MO) to the upper chamber of the inserts above the epithelial cells, incubation for 2 h, and then measuring the absorbance of medium in the lower chamber at 600 nm. The absorbance values were normalized relative to the untreated cells control.

Mouse microarray studies

A total of 20 female 9-week old DBA mice from Jackson's Lab were used for this experiment. Mice were divided into groups of 5, and were inoculated with *B. anthracis* Sterne spores in sterile water i.p. at a concentration of 10^7 spores/mouse. The control group was inoculated with sterile water. After exposure, all mice were euthanized *via* cervical dislocation. Immediately following cervical dislocation, organs were extracted, placed in pre-labeled vials and quickly immersed in liquid nitrogen for storage. To help preserve the quality of the RNA being extracted, entire organs were removed from vials and weighed while still frozen just before homogenization. Homogenization was done using a standard trizol protocol, by placing the entire frozen/thawing organ into a 3 ml glass tissue homogenizer in trizol and immediately homogenizing the organ. RNA was extracted as described. Quality and yield were checked spectrophotometrically, and by running RNA on denaturing gels. All samples were then purified by RNAeasy (Quiagen), and RNA quality was re-checked on denaturing RNA gels. Quantity was

determined by spectrophotometry, and confirmed by denaturing gel intensity. For labeling, 20 µg of total RNA for each experimental day 1, 2 or 3, mouse organ was labeled with Cy5. For control samples, 4 µg of total RNA from each of the 5 mice in a respective control group was combined to yield a 20 µg single, comprehensive control sample for each organ. Each comprehensive control sample was labeled with Cy3. Labeling of control and experimental samples was done by an initial amino-allyl modification of RNA, using 2 µl of random hexamer primer (3 mg/ml) to the 20 µg sample, bringing volume up to 17.9 µl with Rnase-free water, and incubating at 70ºC for 10 min in thermocycler. After placing on ice for 5 min, the sample was centrifuged and the following components of the Invitrogen (Carlsbad, CA) Superscript RT-PCR kit were added: 6 ul 5X First Strand Buffer, 3 µl 0.1M DTT, 1.2 µl 25X aminoallyl-dNTP mix, and 2 µl Superscript II RT (200U/µl). The 25X aminoallyl-dNTP mix contained 5 µl each of 50 mM dATP, dCTP, and dGTP, 3 µl of 50 mM dTTP, and 2 µl of 50 mM aa-dUTP The samples were then incubated O/N at 42ºC in a thermocycler. cDNA synthesis was stopped and RNA was dissolved by adding 20 µl of a 0.5 M NaOH / 50 mM EDTA solution, and incubating samples at 65ºC in a thermocycler for 15 min. Base hydrolysis was stopped by the addition of 20 µl 0.5 M HCl. Samples were then concentrated and purified using a Millipore (Billerica, MA) Micron 30 concentrator, as per the manufacturers instructions, followed by drying in a speed-vac. Cy3/Cy5 Labeling of Aminoalyl-modified cDNA was done by adding 4.5 µl 0.05M sodium bicarbonate buffer ph9 (Coupling Buffer) to the dried samples, followed by 4.5 µl of Cy dye to the appropriate sample (Cy3 for reference samples or Cy5 for experimental samples). Samples were incubated in the dark for 2 hours at RT, and then purified by using a Qiagen (Valencia, CA) Qiaquick PCR purification kit, as per the manufacturers instructions. After purification, samples were dried in a speed vac.

Hybridization was done in a Corning (Corning, NY) hybridization chamber, using a total volume of 49 ul. 38.4 µl of TE was added to the dried samples, followed by 9 µl of 20X SSC, and 1.6 µl of 10% SDS. Samples were heated at 100ºC for 2 min, cooled at RT for 5-10 min, and then all 49 µl was applied to the array slides in a single drop, followed by covering with a 24 X 60 Eire Scientific (Portsmouth, NH) lifterslip. Samples were hybridized O/N at 35ºC, in a Corning hybridization chamber containing 2 drops of 1X SSC. The following morning, arrays were washed

3 times with 2X SSC, 0.2 % SDS at 37ºC 10 min each, followed by washing 5 times with 1X SSC at 37ºC 10 min each. Arrays were then spun at 500 rpm for 10 min, and scanned in a Scanarray as described by the manufacturer.

Chips were developed and produced at Mt. Sinai School of Medicine (Toronto, CA) and consisted of 70-mer oligo arrays, representing 13,824 unique genes of the mouse genome laid down in duplicate on a polylysine surface, yielding a total of approximately 27,648 spots. Realtime PCR was performed on several selected genes to confirm microarray results, using a BIO-RAD (Hurcules, CA) Syber-green kit and components, and a BIO-RAD ICycler.

KEY RESEARCH ACCOMPLISHMENTS

Task 1

This task is completed. Key accomplishments on this task have been reported in the year 2004.

Task 2

Two anthrax proteases, namely M4 elastase and M6 immune inhibitor, have been isolated and purified from *B. anthracis* culture supernatant. Their biochemical properties have been characterized, including:

proteolytic and cytolytic activities

dependence of proteolytic activity on divalent ions

spectrum of inhibitors

degradation of important host extracellular proteins and protease inhibitors

degradation of Synd ectodomain leading to the generation of soluble Synd.

Expression of anthrax recombinant proteases has been continued. New recombinant constructs have been generated and are currently being tested.

It has been shown that other pathogenic factors of *B. anthracis*, in addition to secreted proteases can cause acceleration of host ectodomain shedding of Synd1 and 4, and E-cadherin. These factors include:

pore-forming hemolysin AnlO

phospholipase AnlA

shingomyelinase AnlB

lethal toxin

Individual components of LT, lethal factor and protective antigen are inactive with regard to shedding.

Acceleration Synd-1 and -4 shedding in the circulation of mice challenged with *Bacillus anthracis* (Sterne) spores has been demonstrated. Animal experiments aimed to test ectodomain shedding in different organs of mice during anthrax infectious process are in progress.

It has been demonstrated that Synd shedding in cultured epithelial cells is accompanied by the increase in barrier permeability.

Experiments with pharmacological inhibitors have identified several of the pathways involved in host ectodomain shedding by *B. anthracis* proteins.

Task 3

It has been shown that culture supernatants of atoxigenic anthrax strain, as well as individual secreted proteins of *B. anthracis*, such as AnlB and AnlO can induce TLR-2 signaling in HEK 293 cells transfected with the TLR-expressing constructs.

It has been shown that the AnlO-conditioned medium activated TLR-2. The TLR-2 stimulation correlates with the enzymatic activity of proteases in culture supernatant, and favors the hypothesis that the extracellular domain shedding could contribute to the generation of TLR-signaling proteoglycans, such as soluble Synds.

It has been shown that surface antigens of *B. anthracis* spores induce TLR-2 signaling although factors produced by germinating spores and vegetative cells of the toxigenic Sterne strain effectively inhibit TLR-2 activation.

Analyses of genomic response to anthrax infection in several organs of mice have been carried out. The results have identified candidate genes involved in the innate host response, as well as

genes associated with the progression of disease for further design of novel therapeutic interventions.

Reportable outcomes

Task 1. Synergistic Anti-Toxin/Antibiotic Treatment of Anthrax

a. Perform a synthesis of alkylamino derivatives and test them in *in vitro* and *in vivo* experiments.

b. Based on the findings of the apoptotic activity of lethal toxin (LeTx), evaluate various caspase inhibitors for their ability to inhibit toxin using a murine animal model with various doses and administration schedule.

c. Perform further studies to determine the efficacy of inhibitors combined with immunostimulators that were found to be active against LeTx in *in vitro* experiments with macrophages.

d. Test PrAmBC in mice using different doses, routes of administrations and treatment schedules.

Task 2. Anthrax Protease Inhibitors for Therapy of Late-Stage Inhalational Anthrax

a. Identify proteases produced by *B. anthracis* that are typical of numerous pathogenic organisms using bioinformatics analyses. Choose representative proteases for further study based on their amino acid sequence homology, common structural elements, and shared catalytic groups.

b. Amplify selected protease genes from *B. anthracis* genomic DNA using PCR with specific primers. Perform recombinant expression and purification of selected proteases. Characterize purified proteases for their enzymatic activity and substrate specificity..

c. Study the role of *B. anthracis* secreted proteins from culture supernatants as virulence factors *in vivo*. Determine whether *B. anthracis* proteins are toxic to mice, cause severe hemorrhage or/and increase vascular permeability upon injection into mice. Use human cell culture lines as an alternative *in vitro* model system.

d. Undertake separation of secreted *B. anthracis* proteins from culture supernatants. Characterize hemorrhagic, vascular permeability-enhancing and other potential pathogenic activities of isolated proteins. Wherever possible, identify primary structure of isolated proteins.

e. Evaluate protective efficacy of inhibitors, selected from our analysis of the experimental data on the other bacterial proteases, against *B. anthracis* proteases *in vitro*. Based on the results of the *in vitro* experiments, test the ability of protease inhibitors to protect mice from challenges with purified proteases.

f. Generate polyclonal antibodies against recombinant proteases. Characterize specificity of antibodies towards proteases *in vitro*. Use antibodies as immunological detection tools in the analyses of individual proteases among secreted proteins produced by *B. anthracis*.

g. Evaluate efficacy of antibodies, generated against purified bacterial proteases, in neutralization of *B. anthracis* proteases activity *in vitro*. Based on the results of the *in vitro* experiments, test the ability of protease inhibitors to protect mice from challenges with purified proteases.

Task 3. Toll-like Receptor (TLR) Neutralizing Antibodies and Soluble TLRs as Specific and Broad-Spectrum Protection against Biological Weapons

a. Assess anti-TLR antibodies as specific and broad-spectrum protection against biological weapons. Use TLR-neutralizing antibodies *in vitro* to test their effect on internalization, germination of anthrax spores and intracellular proliferation of vegetative bacilli in macrophages. If neutralizing antibodies block germination of spores and increase viability of macrophages, carry out the experiments on the protective efficacy of antibodies against anthrax infection in mice.

b. Use genetic constructs capable of expressing TLRs to evaluate the possible role of TLRs in the infectious process caused by vaccinia virus in cell culture. Test if TLR-neutralizing antibodies and/or siRNAs can interfere with the vaccinia infections.

c. Generate recombinant constructs for the expression of soluble TLR-2 and -4 in *E. coli* cells. As an alternative, consider the baculovirus expression system. Evaluate the possibility of

isolation and purification of recombinant soluble TLRs from *E. coli* or insect cells. If isolation of soluble TLRs is successful, assess the protective effect of soluble TLRs as potential therapeutic products against biological weapons. Test if administration of soluble TLRs will block interaction between the membrane-bound TLR and the pathogen spore, LeTx or vaccinia virus. Determine if soluble TLR administration will decrease internalization of the invading anthrax spores, block the effect of LeTx and enhance survival of infected macrophages.

d. Test the in vivo role of selected TLRs or TLR adaptors (e.g., MyD88 and TRIF) in the vaccinia virus (TLR2, TLR3 and TLR4) and *B. anthracis* infections (TLR2 and TLR4) using commercially available mice deficient in these TLRs or adaptors.

e. Investigate the role of selected TLRs in the induction of pro-inflammatory cytokines/chemokines using neutralizing anti-TLR antibodies. In case the TLR-stimulating antibodies are available, test if they are able of enhancing the function of immunocompetent cells and elimination the infected agents, such as vaccinia virus or *B. anthracis*.

Conclusions

Secreted virulence factors, in addition to lethal toxin (LT), play important role in anthrax and have previously been identified by us as candidate targets of post-exposure therapies. However, the molecular substrates and specific pathogenic mechanisms of these factors remain largely unknown. During the year 2005, the data generated using epithelial cells in culture and mice challenged with *B. anthracis* spores allow conclude that acceleration of ectodomain shedding by LT, other proteolytic proteins and hemolysins represents a new previously unknown feature of anthrax infection. Secreted pathogenic factors of *B. anthracis* can cause ectodomain shedding likely resulting in protective barriers disruption and tissue penetration by bacilli. In addition, proteolysis of the extracellular matrix can play signaling role as a mediator of lethality perturbing different mechanisms of the host defense response, including the activation of TLRs. Data on pharmacological inhibition of shedding favor a hypothesis that activities of tested bacterial shedding inducers converge on the stimulation of cytoplasmic tyrosine kinases of the Syk family, ultimately leading to activation of cellular sheddase. Both LT and pore-forming hemolysin O

transiently modulate ERK1/2 and p38 MAPK signaling pathways, while JNK pathway seems to be irrelevant to accelerated shedding. The concerted acceleration of shedding by several virulence factors could represent a pathogenic mechanism contributing to hemorrhage, edema and abnormal cell signaling during anthrax infection.

References

Abramova, F.A., Grinberg, L.M., Yampolskaya, O.V., and. Walker D.H. (1993) Pathology of inhalational anthrax in 42 cases from the Sverdlovsk outbreak of 1979. *Proc Natl Acad Sci U S A* **90**:2291-2294.

Aktories, K., and Barbieri, J.T. (2005) Bacterial cytotoxins: targeting eukaryotic switches. *Nat Rev Microbiol* **3**:397-410.

An, S.S., Fabry, B., Mellema, M., Bursac, P., Gerthoffer, W.T., Kayyali, U.S., Gaestel, M., Shore, S.A., and Fredberg, J.J. (2004) Role of heat shock protein 27 in cytoskeletal remodeling of the airway smooth muscle cell. *J Appl Physiol* **96**:1701-1713.

Antelmann, H., Williams, R.C., Miethke, M., Wipat, A., Albrecht, D., Harwood, C.R., Hecker, M. (2005) The extracellular and cytoplasmic proteomes of the non-virulent Bacillus anthracis strain UM23C1-2. *Proteomics* **5**:3684-95.

Arribas, J., Borroto, A. (2002) Protein ectodomain shedding. *Chem Rev* **102**:4627-4638.

Barbey-Morel, C., Perlmutter, D.H. (1991) Effect of pseudomonas elastase on human mononuclear phagocyte alpha 1-antitrypsin expression. *Pediatr Res* **29**:133-40.

Beauvais, D.M., and Rapraeger, AC. (2004) Syndecans in tumor cell adhesion and signaling. *Reprod Biol Endocrinol* **2**: 3-15.

Bernfield, M., Gotte, M., Park, P.W., Reizes, O., Fitzgerald, M.L., Lincecum, J., and Zako, M. (1999) Functions of cell surface heparan sulfate proteoglycans. *Annu Rev Biochem* **68**: 729-777.

Bochud, P.Y., and Calandra, T. (2003) Pathogenesis of sepsis: new concepts and implications for future treatment. *BMJ* **326**:262-266

Botta, M., Manetti, F., and Corelli, F. (2000) Fibroblast growth factors and their inhibitors. *Curr Pharm Des* **6**(18):1897-1924.

Charlton, S., Moir, A.J., Baillie, L., Moir, A. (1999) Characterization of the exosporium of Bacillus cereus. *J Appl Microbiol* **87**:241-5

Duesbery, N.S., Webb, C.P., Leppla, S.H., Gordon, V.M., Klimpel, K.R., and Copeland, T.D., *et al.* (1998) Proteolytic inactivation of MAP-kinase-kinase by anthrax lethal factor. *Science* **280**: 734-737.

Firth, J.D., Putnins, E.E., Larjava, H., and Uitto, V.J. (2001) Exogenous phospholipase C stimulates epithelial cell migration and integrin expression *in vitro*. *Wound Repair Regen* **9**:86-94.

Fitzgerald, M.L., Wang, Z., Park, P.W., Murphy, G., and Bernfield, M. (2000) Shedding of syndecan-1 and -4 ectodomains is regulated by multiple signaling pathways and mediated by a TIMP-3-sensitive metalloproteinase. *J Cell Biol* **148**: 811-824.

Fouquet, S., Lugo-Martinez, V.H., Faussat, A.M., Renaud, F., Cardot, P., Chambaz, J., Pincon-Raymond, M., Thenet, S. (2004) Early loss of E-cadherin from cell-cell contacts is involved in the onset of Anoikis in enterocytes. *J Biol Chem* **279**:43061-43069.

Grinberg, L.M., Abramova, F.A., Yampolskaya, O.V, Walker, D.H. and Smith, J.H. (2001) Quantitative pathology of inhalational anthrax I: quantitative microscopic findings. *Mod Pathol* **14**: 482-495.

Higashiyama, S., and Nanba, D. (2005) ADAM-mediated ectodomain shedding of HB-EGF in receptor cross-talk. *Biochim Biophys Act* **1751**:110-117

Hirai S., Izawa M., Osada S., Spyrou G., Ohno S. (1996) Activation of the JNK pathway by distantly related protein kinases, MEKK and MUK. *Oncogene* **12**(3):641-650.

Hooper, N.M., and Turner, A.J. (1999) Membrane protein secretases. *Biochem Soc Trans* **27**: 211-257.

Huffman, D.L., Abrami, L., Sasik, R., Corbeil, J., Goot, F., and Aroian, R.(2004) Mitogen-activated protein kinase pathways defend against bacterial pore-forming toxins. *Proc Nat Acad Sci USA* **101**:10995-11000

Inglesby, T.V., O'Toole, T., Henderson, D.A., Bartlett, J.G., Ascher, M.S., Eitzen, E. *et al.,*. (2002) Anthrax as a biological weapon: updated recommendations for management. *JAMA* **287**:2236-2252.

Ivanov, A.I., Nusrat, A., and Parkos, C.A. (2005) Endocytosis of the apical junctional complex: mechanisms and possible roles in regulation of epithelial barriers. *Bioessays* **27**: 356-365.

Jaffray, C., Yang, J., and Norman, J. (2000a). Elastase mimics pancreatitis-induced hepatic injury via inflammatory mediators. *J Surg Res* **90**:95-102.

Jaffray C, Yang J, Carter G, Mendez C, Norman J. (2000b). Pancreatic elastase activates pulmonary nuclear factor κB and inhibitory κB, mimicking pancreatitis-associated adult respiratory distress syndrome. *Surgery* **128**:225-137.

Johansen, T., Bjorkoy, G., Overvatn, A., Diaz-Meco, M.T., Traavik, T., and Moscat, J. (1994) NIH 3T3 cells stably transfected with the gene encoding phosphatidylcholine-hydrolyzing phospholipase C from Bacillus cereus acquire a transformed phenotype. *J.Mol Cell Biol* **14**:646-654.

Johnson GB, Brunn GJ, and Platt JL. (2003). Activation of mammalian Toll-like receptors by endogenous agonists. *Crit Rev Immunol* **23**:15-44

Johnson, G.B., Brunn, G.J., and Platt, J.L. (2004) An endogenous pathway to systemic inflammatory response syndrome (SIRS)-like reactions through toll-like receptor 4. *J Immun* **172**: 20-24.

Ikei, S., Ogawa, M., and Yamaguchi, Y. (1998) Blood concentrations of polymorphonuclear leucocyte elastase and interleukin-6 are indicators for the occurrence of multiple organ failures at the early stage of acute pancreatitis. *J Gastroenterol Hepatol* **13**:127-138.

Kassam, A., Der, S.D., Mogridge, J. (2005) Differentiation of human monocytic cell lines confers susceptibility to Bacillus anthracis lethal toxin. *Cell Microbiol* **7**:281-292

Kato, M., Saunders, S., Nguyen, H., and Bernfield, M. (1995) Loss of cell surface syndecan-1 causes epithelia to transform into anchorage-independent mesenchyme-like cells. *Mol Biol Cell.* **6**:559-576.

Kawabata, K., Hagio, T., and Matsuoka, S. (2002) The role of neutrophil elastase in acute lung injury. *Eur J Pharmacol* **451**:1-14.

Keim, V., Teich, N., Reich, A., Fiedler, F., and Mossner, J. (1997) Polyclonal pancreatic elastase assay is superior to monoclonal assay for diagnosis of acute pancreatitis. *Clin Chem* **43**:2339-2340.

Keradmand, F., and Werb, Z. (2002) Shedding light on sheddases: role in growth and development. *BioEssays* **24**:8-12.

Khan, M.M., Shibuya, Y., Kambara, T., and Yamamoto, T. (1995) Role of alpha-2-macroglobulin and bacterial elastase in guinea-pig pseudomonal septic shock. *Int J Exp Pathol* **76**:21-8.

Kevil, C.G., Oshima, T., and Alexander, J.S. (2001) The role of p38 MAP kinase in hydrogen peroxide mediated endothelial solute permeability. *Endothelium* **8**:107-116.

Kirby, J.E. (2004) Anthrax lethal toxin induces human endothelial cell apoptosis. *Infect Immun* **72**: 430-439.

Klichko, V.I., Miller, J., Wu, A., Popov, S.G., and Alibek, K. (2003) Anaerobic induction of Bacillus anthracis hemolytic activity. *Biochem Biophys Res Commun* **303**: 855-862.

Li, L., and Chaikof, E.L. (2002) Mechanical stress regulates syndecan-4 expression and redistribution in vascular smooth muscle cells. *Arterioscler Thromb Vasc Biol* **22**:61-68.

Mahabeleshwar, G.H., and Kundu, G.C. (2003) Syk, a protein-tyrosine kinase, suppresses the cell motility and nuclear factor kappa B-mediated secretion of urokinase type plasminogen activator by inhibiting the phosphatidylinositol 3'-kinase activity in breast cancer cells. *J Biol Chem* **278**: 6209-6221.

McCain, D.F., Wu, L., Nickel, P., Kassack, M.U., Kreimeyer, A., Gagliardi, A., Collins, D.C., and Zhang, Z.Y.(2004) Suramin derivatives as inhibitors and activators of protein-tyrosine phosphatases. *J Biol Chem* **279**:14713-14725.

McMullen, M.E., Bryant, P.W., Glembotski, C.C., Vincent, P.A., and Pumiglia, K.M. (2005) Activation of p38 has opposing effects on the proliferation and migration of endothelial cells. *J Biol Chem* **280**:20995-21003.

Meng, G., Rutz, M., Schiemann, M., Metzger, J., Grabiec, A., Schwandner, R., Luppa, P.B., Ebel, F., Busch, D.H., Bauer, S., Wagner, H., and Kirschning, C.J. (2004) Antagonistic antibody prevents toll-like receptor 2-driven lethal shock-like syndromes. *J Clin Invest* **113**:1473-81.

Mikshis, N.I., Eremin, S.A., and Bolotnikova, M.F. (1999) Correlation of the virulence of Bacillus anthracis with expression of signs, coded for by chromosomal genes. *Mol Gen Mikrobiol Virusol* **4**: 25-28.

Moayeri, M., and Leppla, S,H. (2004) The roles of anthrax toxin in pathogenesis. *Curr Opin Microbiol* **7**:19-24

Moayeri, M., Haines, D., Young, H.A., and Leppla, S.H. (2003) Bacillus anthracis lethal toxin induces TNF-alpha-independent hypoxia-mediated toxicity in mice. *J Clin Invest* **112**: 670-682

Mun-Bryce, S., and Rosenberg, G.A. (1998) Matrix metalloproteinases in cerebrovascular disease. *J Cereb Blood Flow Metab* **18**: 1163-1172.

Narasaki, R., Kuribayash,i H., Shimizu, K., Imamura, D., Sato, T., and Hasumi, K. (2005) Bacillolysin MA, a novel bacterial metalloproteinase that produces angiostatin-like fragments from plasminogen and activates protease zymogens in the coagulation and fibrinolysis systems. *J Biol Chem* **28014**:14278-14287.

Nguyen, A., Chen, P., and Cai, H. (2004) Role of CaMKII in hydrogen peroxide activation of ERK1/2, p38 MAPK, HSP27 and actin reorganization in endothelial cells. *FEBS Lett* **572**:307-313.

Park, P.W., Pier, G.B., Preston, M.J., Goldberger, O., Fitzgerald, M.L., and Bernfield, M. (2000) Syndecan-1 shedding is enhanced by LasA, a secreted virulence factor of Pseudomonas aeruginosa.*J Biol Chem* **275**: 3057-3064.

Park, P.W., Pier, G.B., Hinkes, M.T., and Bernfield, M. (2001) Exploitation of syndecan-1 shedding by Pseudomonas aeruginosa enhances virulence. *Nature* **411**: 98-102.

Park, P.W., Foster, T.J., Nishi, E., Duncan, S.J., Klagsbrun, M., and Chen, Y. (2004) Activation of syndecan-1 ectodomain shedding by Staphylococcus aureus alpha-toxin and beta-toxin. *J Biol Chem* **279**: 251-258.

Park, J.M, Ng, V.H., Maeda, S., Rest, R.F., and Karin, M. (2004b) Anthrolysin O and other gram-positive cytolysins are toll-like receptor agonists. *J Exp Med* **200**: 1647-1655.

Popov, S.G., Popova, T.G., Hopkins, S., Weinstein, R.S., MacAfee, R., Fryxell, K.J., Chandhoke, V., Bailey, C., and Alibek, K. (2005) Effective antiprotease-antibiotic treatment of experimental anthrax. *BMC Infect Dis* **5**: 25-39.

Ralevic, V. and Burnstock, G. (1998) Receptors for purines and pyrimidines. *Pharmacol Rev* **50**:413-92.

Read, T.D., Peterson, S.N., Tourasse, N., Baillie, L.W., Paulsen, I.T., and Nelson, K.E., *et al.* (2003) The genome sequence of Bacillus anthracis Ames and comparison to closely related bacteria. *Nature* **423**:81-86.

Sawai, T., Usui, N., Dwaihy, J., Drongowski, R.A., Abe, A., Coran, A.G., and Harmon, C.M. (2000) The effect of phospholipase A2 on bacterial translocation in a cell culture model. *Pediatr Surg Int* **16**:262-266.

Salles, I.I., Tucker, A.E., Voth, D.E., and Ballard, J.D. (2003) Toxin-induced resistance in Bacillus anthracis lethal toxin-treated macrophages. *Proc Nat Acad Sci USA* **100**: 12426-12431.

Shannon, J.G., Ross, C.L., Koehler, T.M., and Rest, R.F. (2003) Characterization of anthrolysin O, the Bacillus anthracis cholesterol-dependent cytolysin. *Infect Immun* **71**: 3183-3189.

Smith, H., Keppie, J., and Stanley, J.L. (1955). The chemical basis of the virulence of *Bacillus anthracis*. V. The specific toxin produced by *B. anthracis in vivo*. *Br J Exp Pathol* **36**:460-472.

Smith, H., and Stoner, H.B. (1967) Anthrax toxic complex. *Fed Proc* **26**:1554-1557.

Sugimoto K., Ohata M., Miyoshi J., Ishizaki H., Tsuboi N., Masuda A., Yoshikai Y., Takamoto M., Sugane K., Matsuo S., Shimada Y., Matsuguchi T. (2004) A serine/threonine kinase, Cot/Tpl2, modulates bacterial DNA-induced IL-12 production and Th cell differentiation. *J Clin Invest* **114**(6):857-866.

Vasconcelos, D., Barnewall, R., Babin, M., Hunt, R., Estep, J., Nielsen, C., Carnes, R., and Carney, J. (2003) Pathology of inhalation anthrax in cynomolgus monkeys (Macaca fascicularis). *Lab Invest* **83**:1201-1209.

Song M, Zaninovic V, Kim D, Gukovsky I, Gukovskaya A, Kang K, Pandol S.1999. Amelioration of rat cerulein pancreatitis by guamerin-derived peptide, a novel elastase inhibitor. Pancreas 18:231

Stoker, A.W. (2005) Protein tyrosine phosphatases and signalling. *J Endocrinol* **185**:19-33.

Timmermann, M., and Hogger, P. (2005) Oxidative stress and 8-iso-prostaglandin F(2alpha) induce ectodomain shedding of CD163 and release of tumor necrosis factor-alpha from human monocytes. *Free Radic Biol Med* 2005 **39**:98-107.

Warfel, J.M., Steele, A.D., and D'Agnillo, F (2005) Anthrax lethal toxin induces endothelial barrier dysfunction. *Am J Pathol* **166**:1871-1881.

Weighardt, H. *et al.* (2002) Cutting edge: myeloid differentiation factor 88 deficiency improves resistance against sepsis caused by polymicrobial infection. *J Immunol* **169**:2823-2827.

Wilcox-Adelman, S.A., Denhez, F., Iwabuchi, T., Saoncella, S., Calautti, E., Goetinck, P.F., and Glycoconj, J. (2002) Syndecan-4: dispensable or indispensable? **19**:305-13.

Wong, W.S., and Leong, K.P. (2004) Tyrosine kinase inhibitors: a new approach for asthma. *Biochim Biophys Acta* **1697**: 53-69.

Wright, G.G., Hedberg, M.A., and Slein, J.B: (1954) Studies on immunity in anthrax. III. Elaboration of protective antigen in a chemically-defined, non-protein medium. *J Immunol* , **72:**263-269

Yamano, M., Miyata, K., and Yamada, T. (1998) Protective effect of a pancreatic elastase inhibitor against a variety of acute pancreatitis in rats. *Jpn J Pharmacol* **77**:1-13.

Yanagishita. M., Hascall, V.C. (1992) Cell surface heparan sulfate proteoglycans. *J Biol Chem* **267**:9451-9454.

Zhang, Y.L., Keng, Y.F., Zhao, Y., Wu, L., and Zhang, Z.Y. (1998) Suramin is an active site-directed, reversible, and tight-binding inhibitor of protein-tyrosine phosphatases. *J Biol Chem* **15**:12281-12287.

Figures

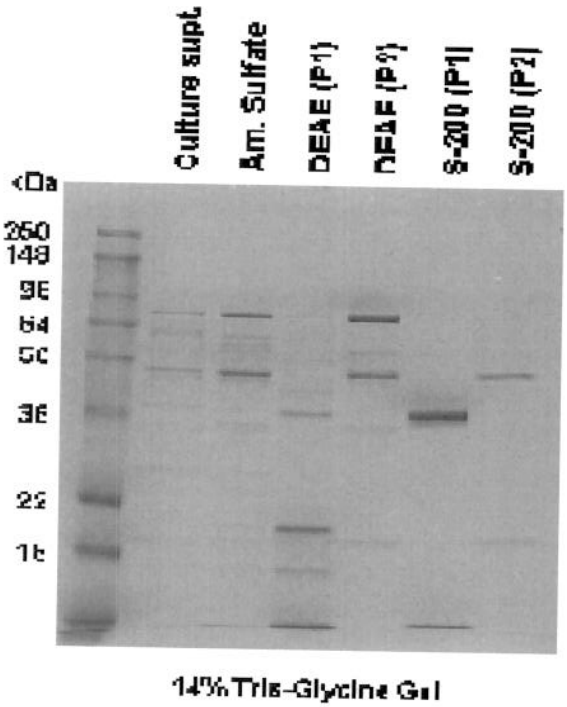

Fig.1. SDS-PAGE of purified proteases

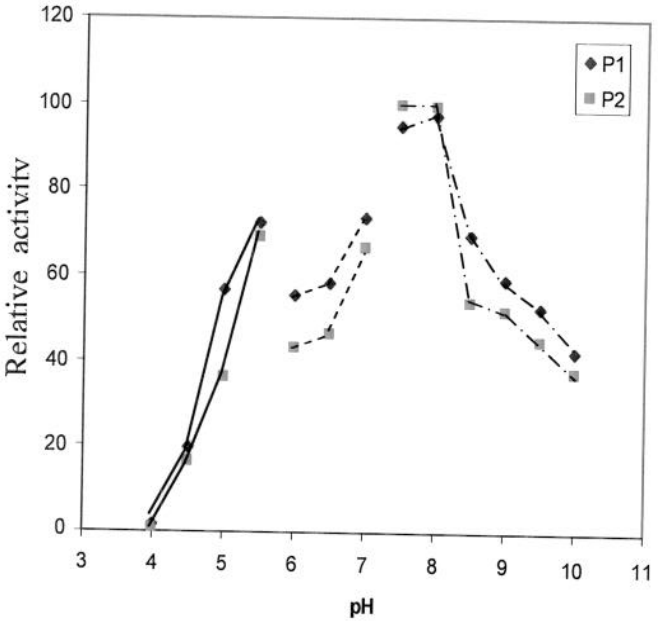

Fig. 2. Effect pH on the caseinolytic activity of proteases. The following buffer solution were used: 50 mM NaOAc-AcOH (pH 4 - 5.5); 50 mM MES-NaOH (pH 6 – 7), : 50 mM Tris-HCl, 100 mM NaCl (pH 7.5- 10)

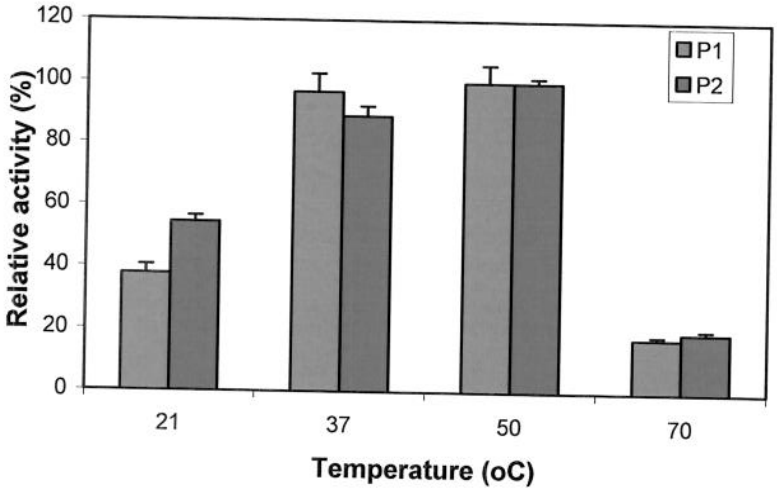

Fig. 3. Effect of temperature on the caseinolytic activity of proteases.

Fig. 4. Host protein cleavage by isolated proteases

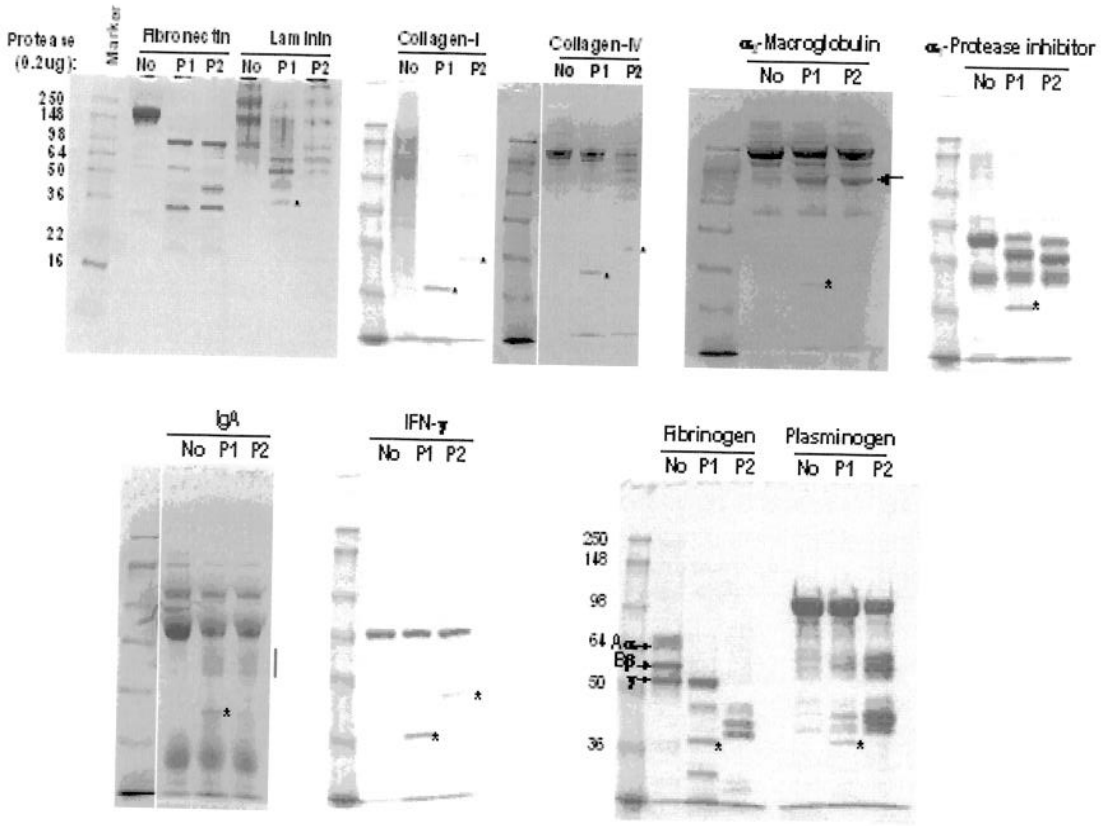

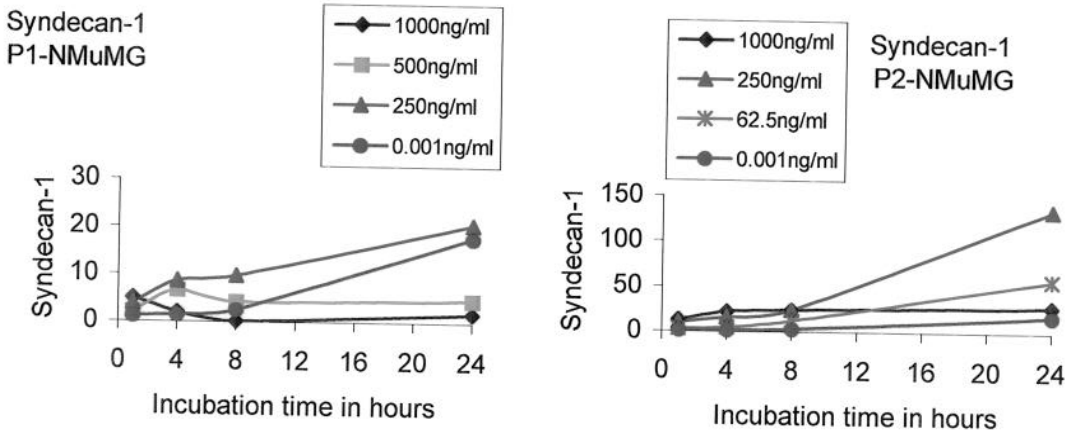

Fig. 5. Syndecan-1 shedding by isolated proteases from NMuMG cells

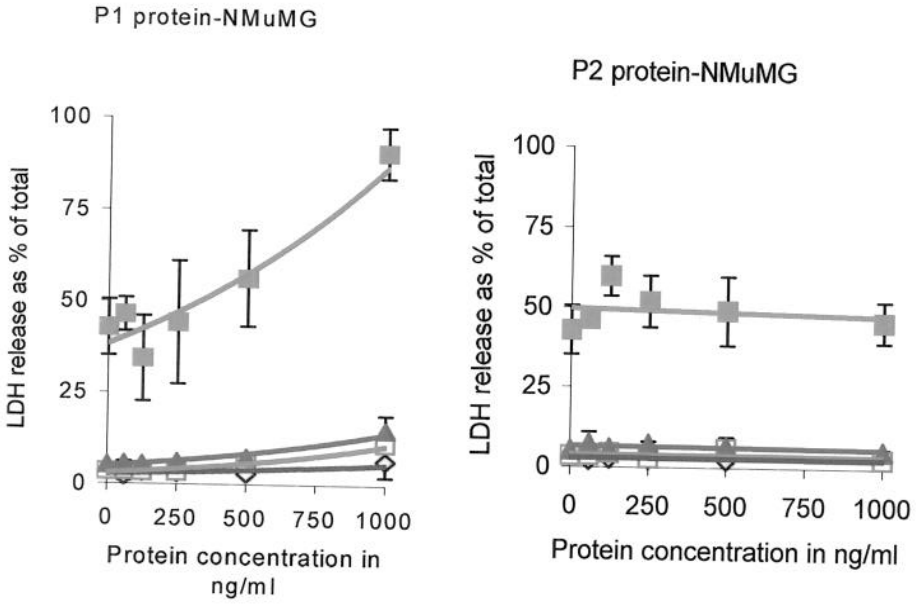

Fig. 6. NMuMG cell lysis by isolated proteases. , 1h (diamonds); 4h (open squares); 8h (triangles);, 24h (filled squares) incubation with proteases.

A. Heparin affinity chromatography

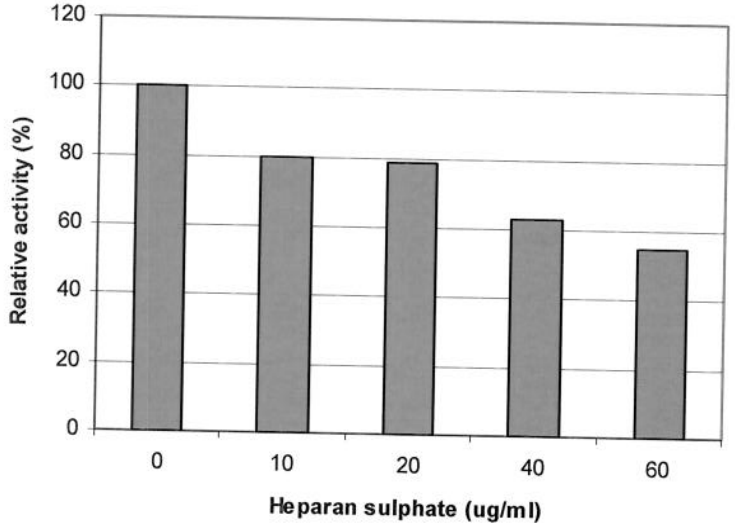

B. Inhibition of protease P1 by heparan sulfate

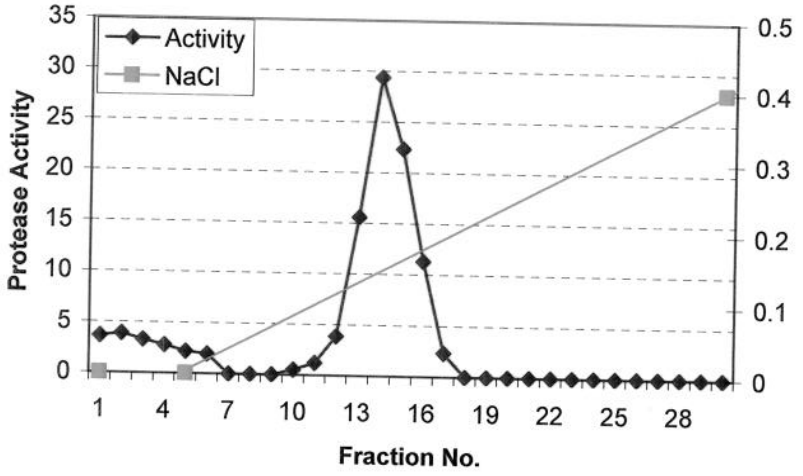

Fig. 7. Interaction of P1 protease with heparin and heparan sulfate.

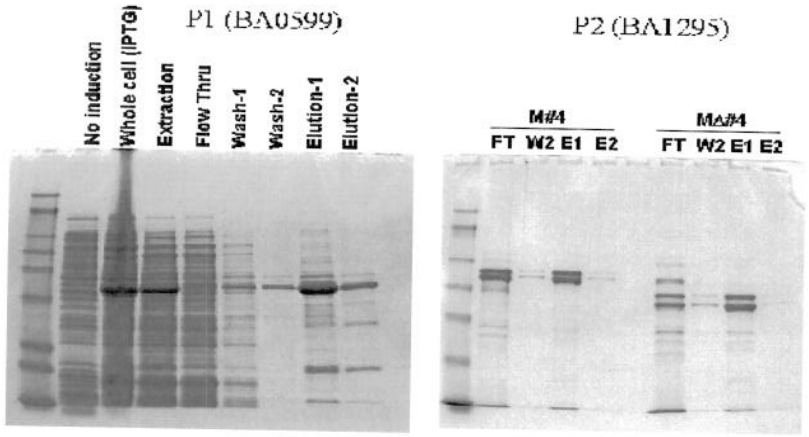

Fig. 8. Isolation of recombinant proteases from *E.coli* cells. Left panel, P1; right panel, P2.

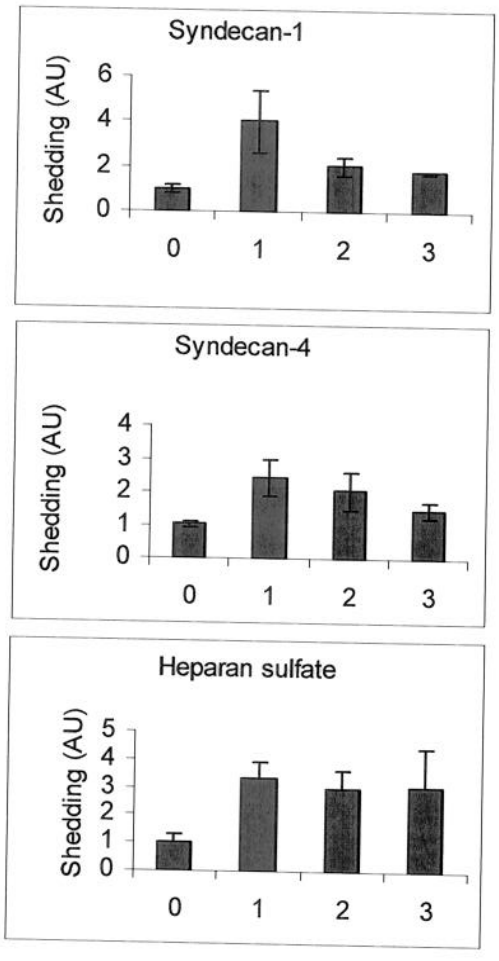

Fig. 9. Synd1, Synd4 and a total heparan sulfate content in the bloodstream of mice challenged with 30 LD_{50} of Sterne strain spores intraperitoneally. The serum samples were blotted in duplicates onto three membranes, which were used separately for immunodetection of Synd1 with antibody 281-2, Synd4 with antibody KY/8.2, and total heparan sulfate with antibody MAB-2040. Graphs represent average fold increases over control in concentrations of indicated substances calculated for two mice at the day of challenge, three mice at each day 1 and 2, and two mice at day 3. Error bars indicate 95% confidence intervals.

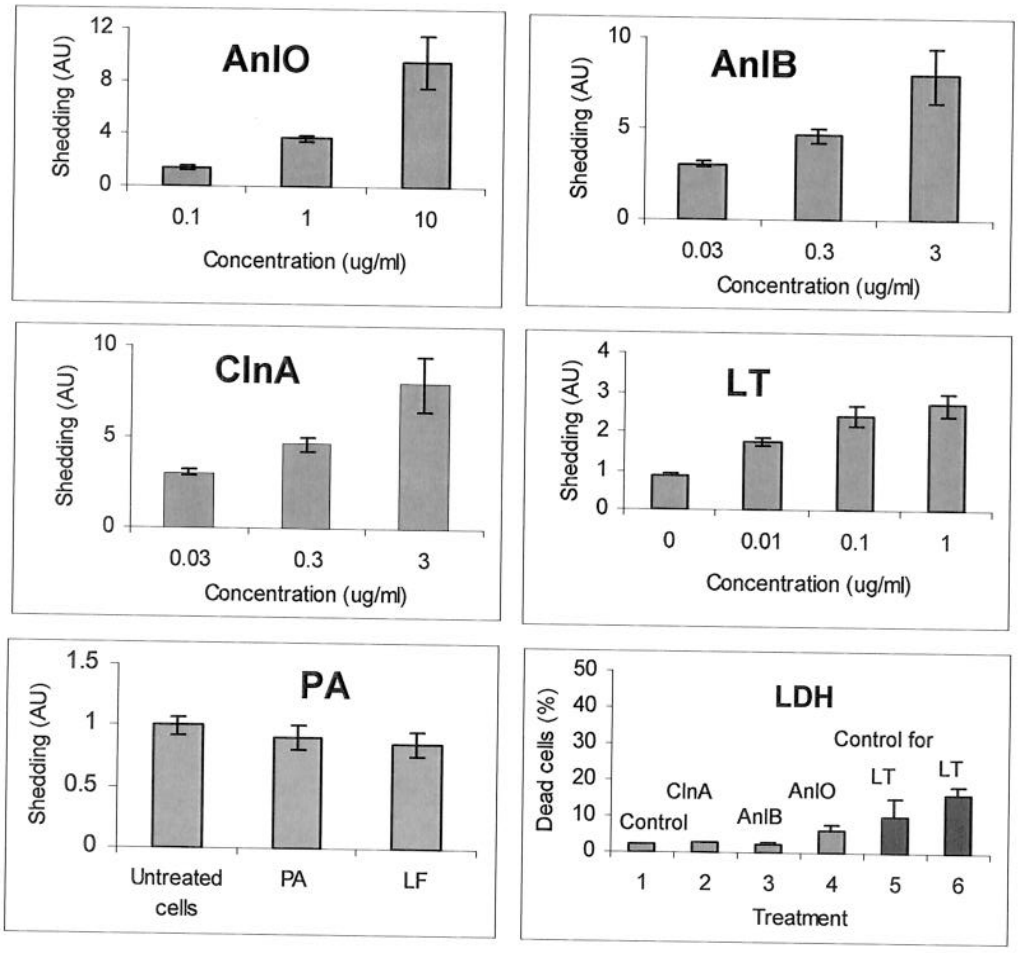

Fig. 10. Synd1 shedding from NMuMG cells in culture after treatment with *B. anthracis* proteins in the presence of 1% FCS for 4 h (24 h in the case of LT, PA and LF). The lower right panel shows cell death measured after 4h as LDH release for untreated cells (1), 1 µg/ml ClnA (2), 1 µg/ml AnlB (3), 0.1 µg/ml AnlO (4), untreated cells after 24 h (5), 1 µg/ml LT after 24 h (6). Error bars represent 95% confidence intervals.

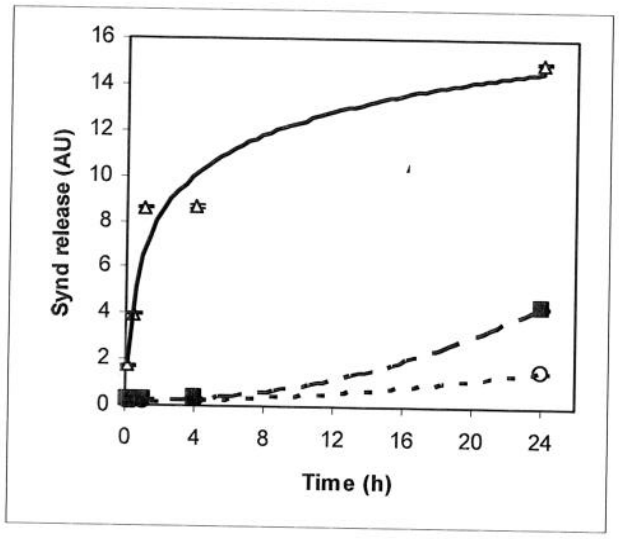

Fig. 11. Time cause of Synd1 release from NMuMG cells transferred into 1% FCS media and challenged with 1 µg/ml of either AnlO (triangles), or LT (squares). Control cells were left untreated (circles). Each measurement corresponds to average of three culture wells.

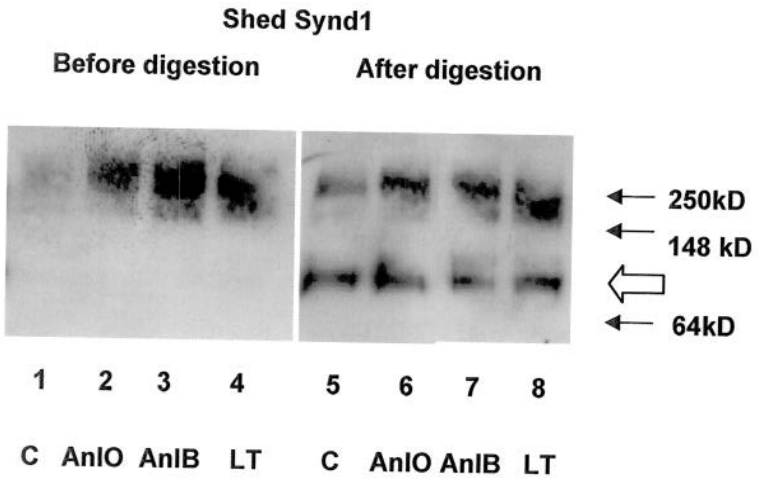

Fig. 12. Western blot of Synd1 shed from NMuMD cells by *B. anthracis* proteins in presence of 1% FCS for 24h. Synd1 from culture supernatants was partially purified using DEAE ion exchange chromatography and analyzed before (lanes 1 to 4) and after (lanes 5 to 8) partial digestion for 5 h with both heparinase II (10 mU/ml) and chondroitin sulfate ABC lyase (20 mU/ml) to remove glycosaminoglycan chains. For digestion the amount of total protein in each reaction was adjusted approximately equal. Gel lanes correspond to untreated cells (1, 5) and cells challenged with: 0.1 µg/ml of Aln O for 4h (2, 6); 1 µg/ml of AlnB for 4h (3, 7); 1 µg/ml of LT for 24 h (4, 8). Synd1 core protein appears as a band of approximately 80 kD (open arrow).

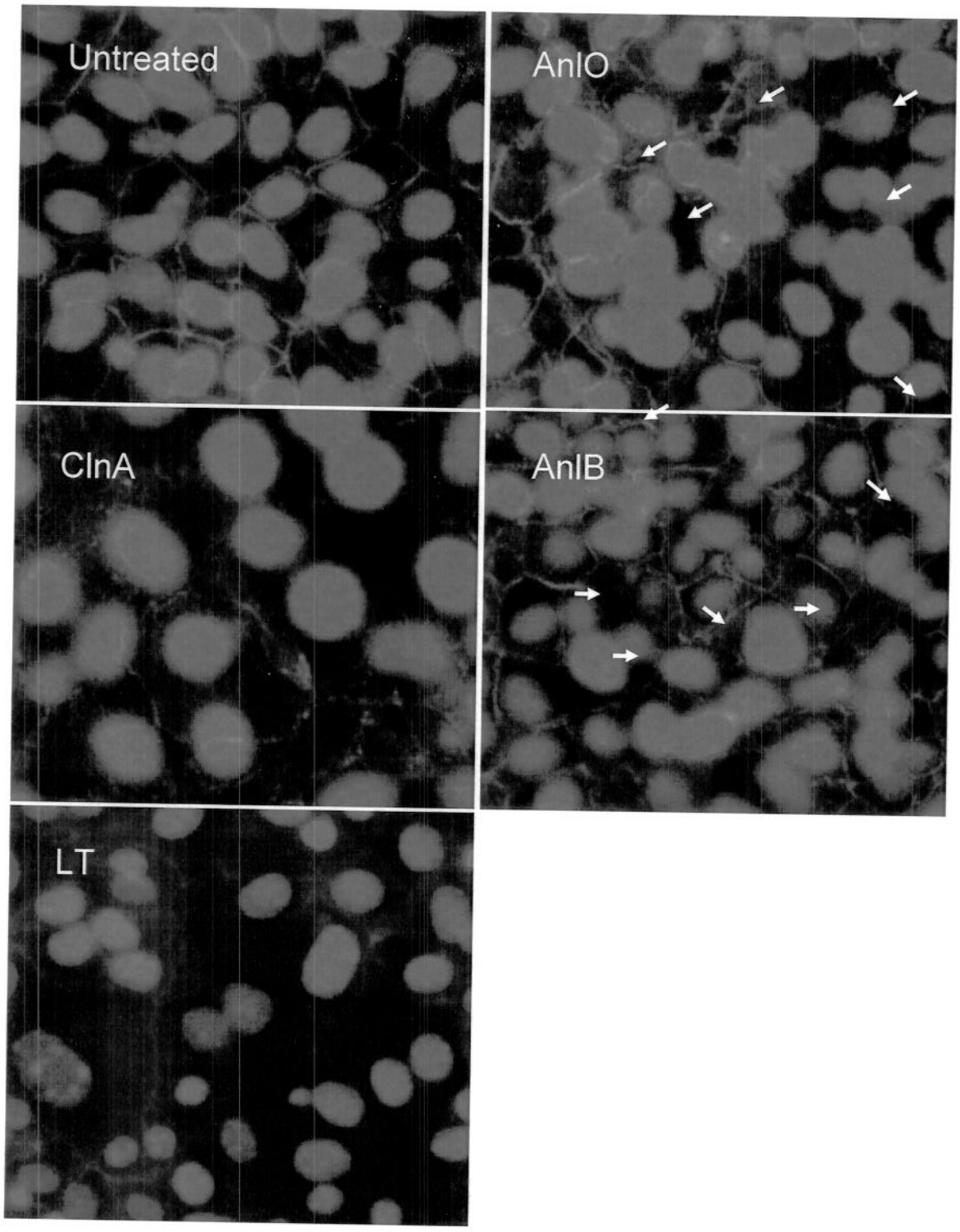

Fig. 13. Immunohistochemical detection of E-cadherin in monolayers of NMuMG cells after treatment with *B. anthracis* proteins (1 µg/ml each for 16 h). Nuclei are stained blue with Dapi, and E-cadherin is stained green with FITC-conjugated anti-Synd1 antibody. 40x magnification. In the case of AnlO and AnlB, arrows indicate some of the most damaged areas.

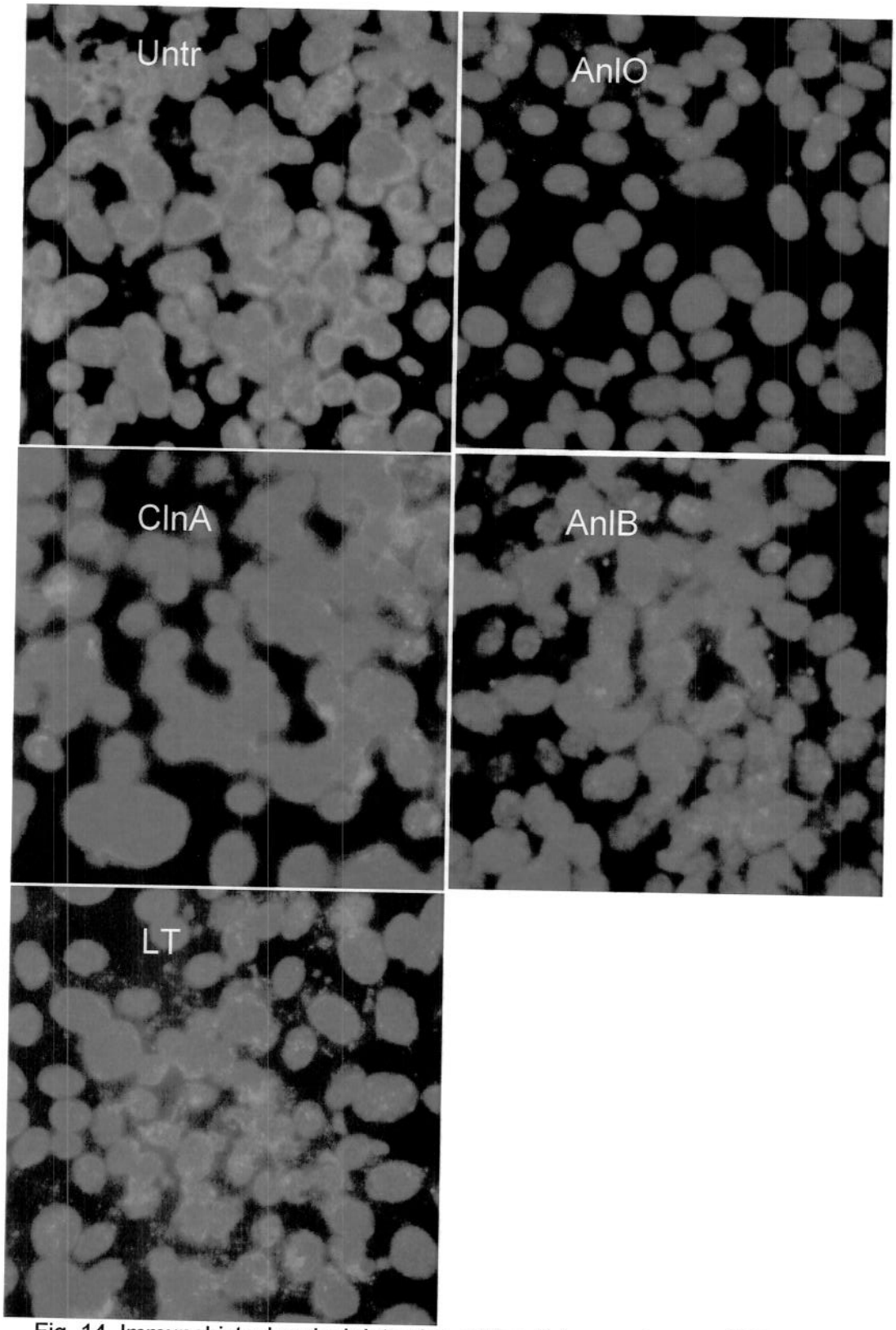

Fig. 14. Immunohistochemical detection of Synd1 in monolayers of NMuMG cells after treatment with *B. anthracis* proteins (1 μg/ml each for 24 h). Nuclei are stained blue with Dapi, and Synd1 is stained green with FITC-conjugated anti-Synd1 antibody. 40x magnification.

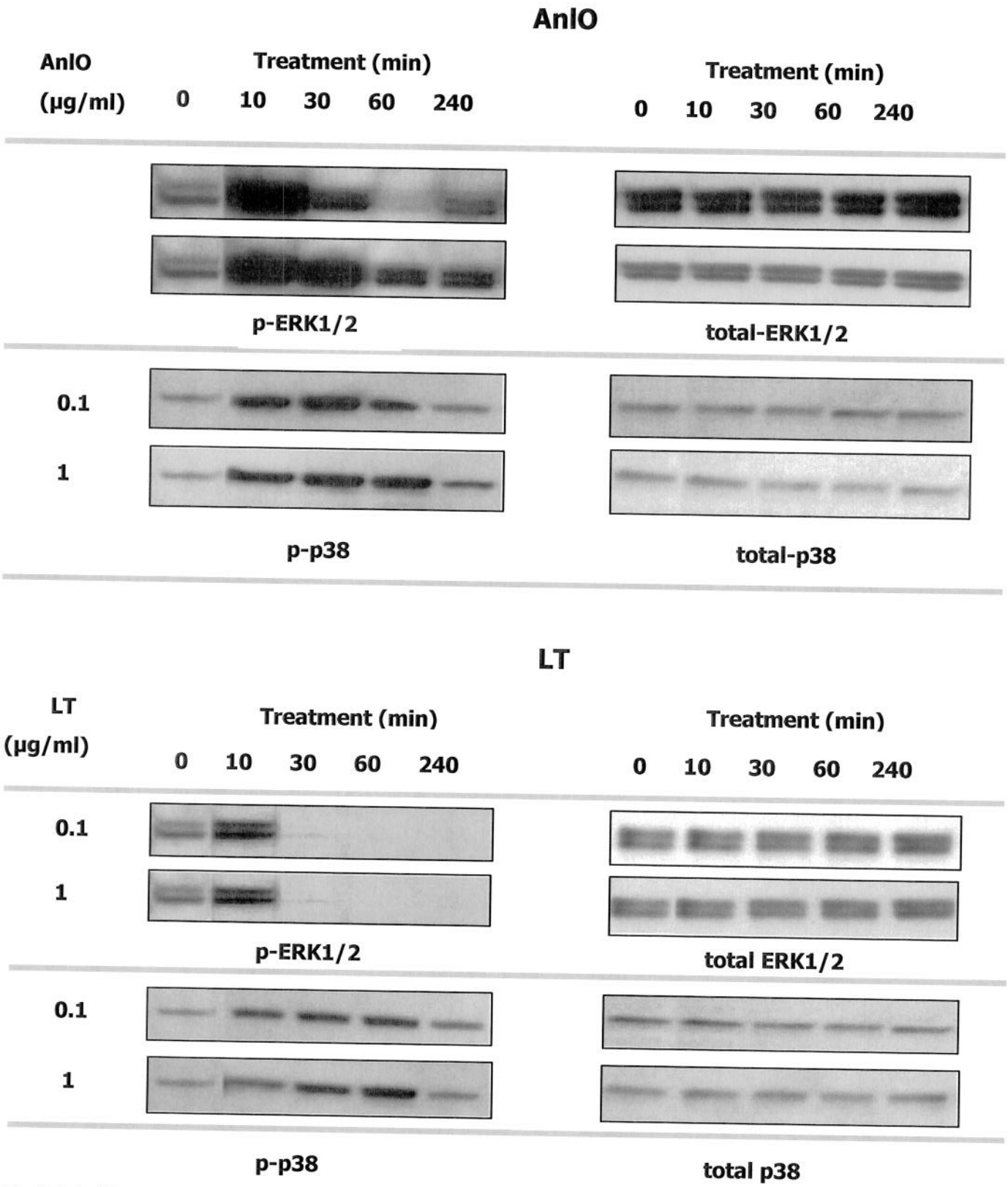

Fig.15. AnlO and LT cause transient phosphorylation of ERK1/2 and p38 in NMuMG epithelial cells. Cells were transferred into growth media with 1% FCS, treated with either AnlO or LT for indicated periods of time, and lysed. Western blots were probed with phosphorylation-specific antibodies against ERK1/2 and p38.

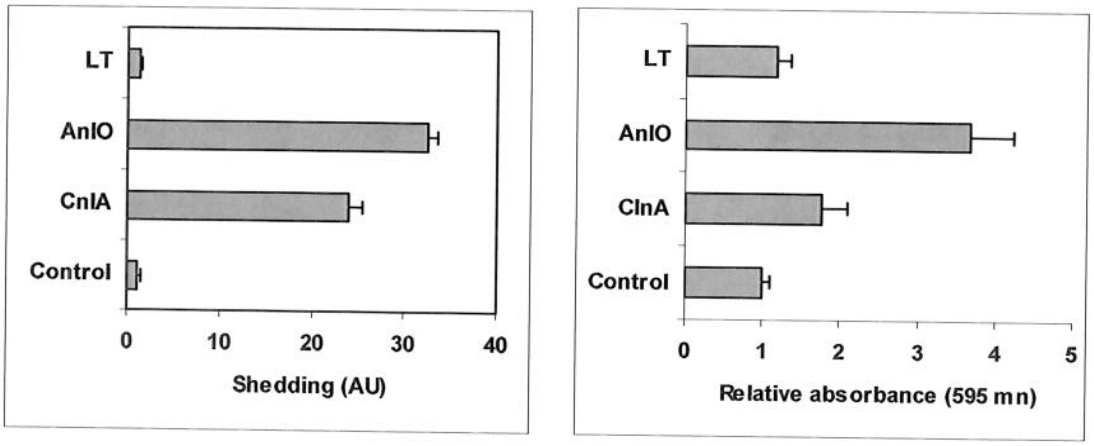

Fig. 16. Shedding of Synd1 into culture supernatants (A) and changes in barrier permeability (B) for HSAECs treated with the hemolytic proteins and LT. The cells initially confluent on a 12mm insert (Costar, 3.0 μm pores) were treated with 1 μg/ml of each protein for 4 h in 1% FCS media. After treatment the change in barrier permeability was tested as increase in the absorbance of Blue Dextran 2000 added for 2 h to the culture media in the top chamber and detected in the lower chamber, in comparison with untreated cells. Error bars indicate confidence intervals (p=0.05); 3 culture plate wells were used for each measurement.

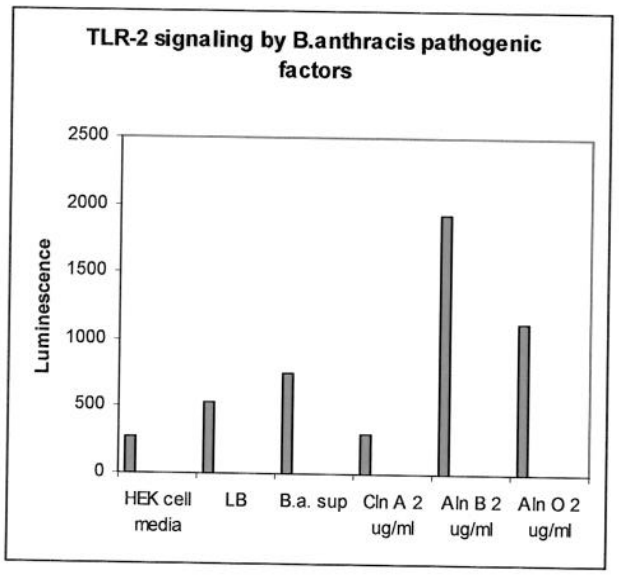

Fig.17. TLR-2 response in HEK 293 cells upon treatment with *B. anthracis* pathogenic factors: culture supernatant (B.a. sup) diluted 8-fold, ClnA, AnlB, and AnlO. Treatment was carried out in presence of 10% FCS for 24 h. Controls include bacterial (LB) and HEK cell media. Luminescence is shown in arbitrary units.

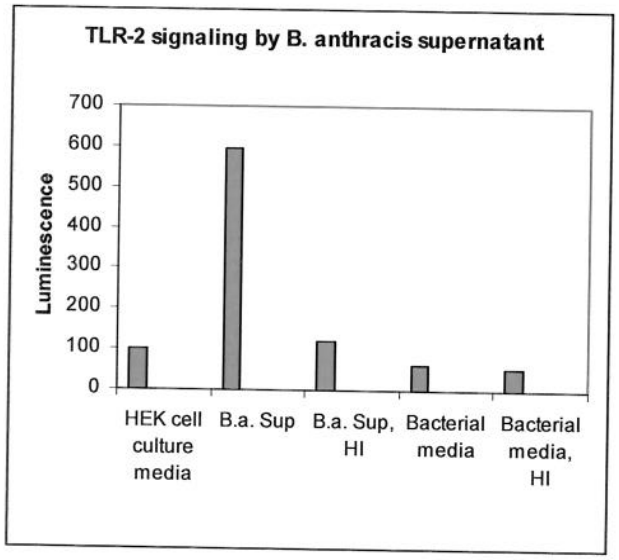

Fig. 18. TLR-2 response in HEK 293 cells upon treatment with *B. anthracis* culture supernatant (B.a. sup) diluted 8-fold before and after heat inactivation (HI). Treatment was carried out in presence of 0.5% FCS for 24 h. Controls include bacterial and HEK cell media. Luminescence is shown in arbitrary units.

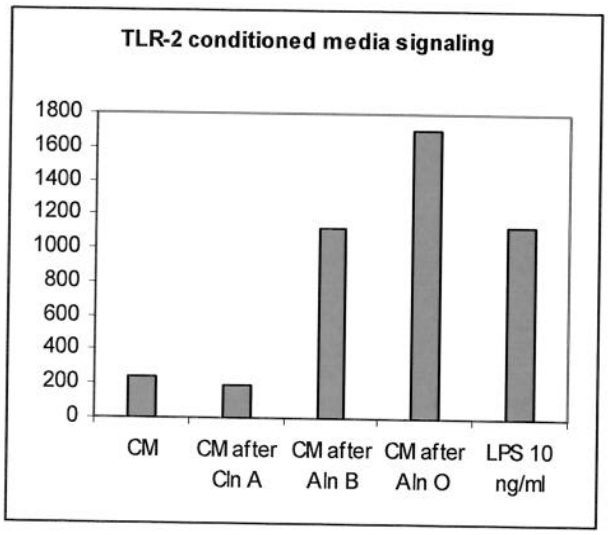

Fig. 19. TLR-2 response in HEK 293 cells in presence of 10% FCS after 24 h induced by *B. anthracis* hemolysins indirectly through conditioned medias, which were obtained after incubation of NMuMG cells with 10 µg/ml of a particular hemolysin in presence of 10% FCS for 4 h. Controls include bacterial and HEK cell media. Luminescence is shown in arbitrary units.

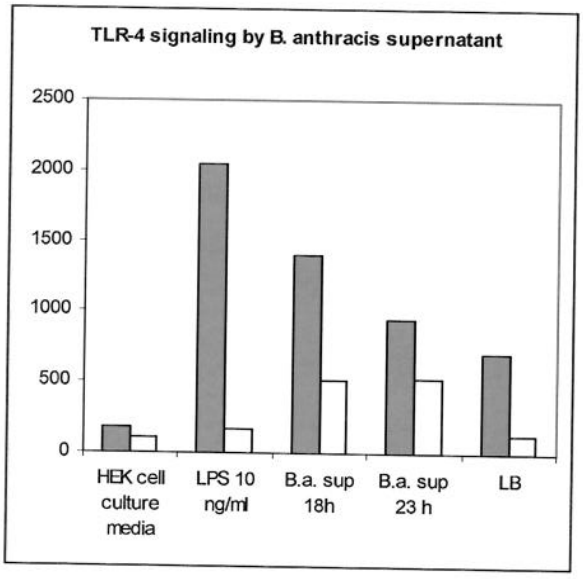

Fig.20. TLR-4 response in HEK 293 cells upon treatment with *B. anthracis* culture supernatant (B.a. sup) diluted 8-fold in presence (open bars) and in absence (filled bars) of 25 µg/ml polymyxin. Treatment was carried out in presence of 10% FCS for 24 h. Controls include bacterial and HEK cell media, and 1 µg/ml LPS. Luminescence is shown in arbitrary units.

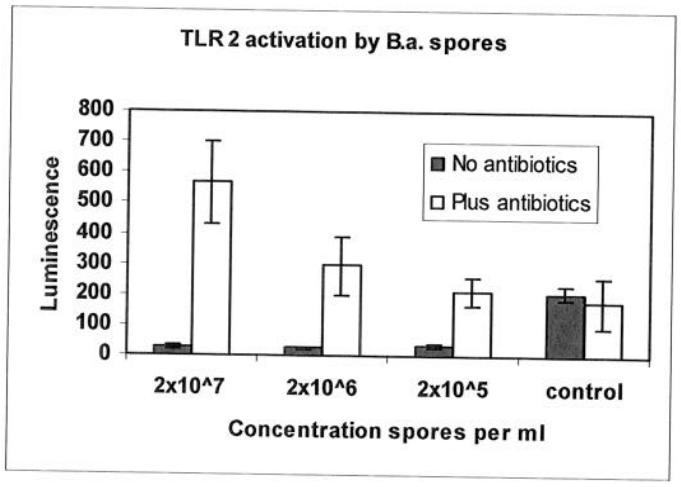

Fig. 21. TLR-2 response in HEK 293 cells upon treatment with *B. anthracis* Sterne spores in presence (open bars) and in absence (filled bars) of penicillin/streptomycin (100 IU/100 µg/ml) in 1% FCS culture media for 18 h. Controls include HEK cell media. Luminescence is shown in arbitrary units.

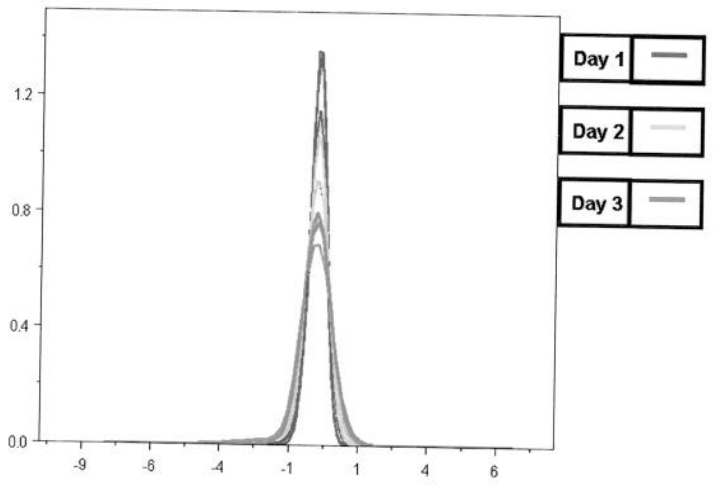

a.

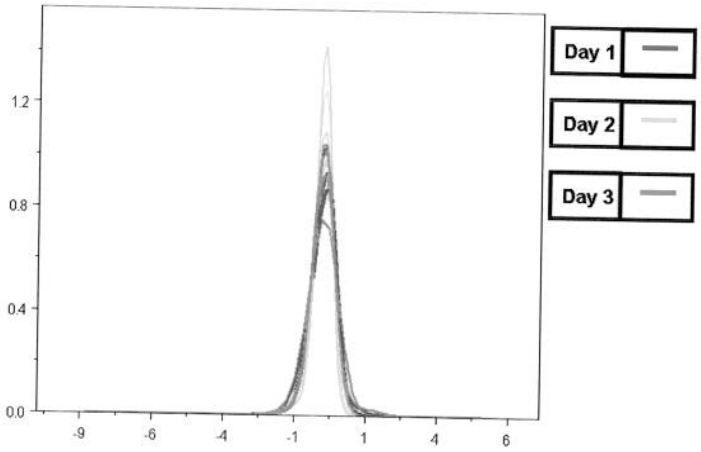

b

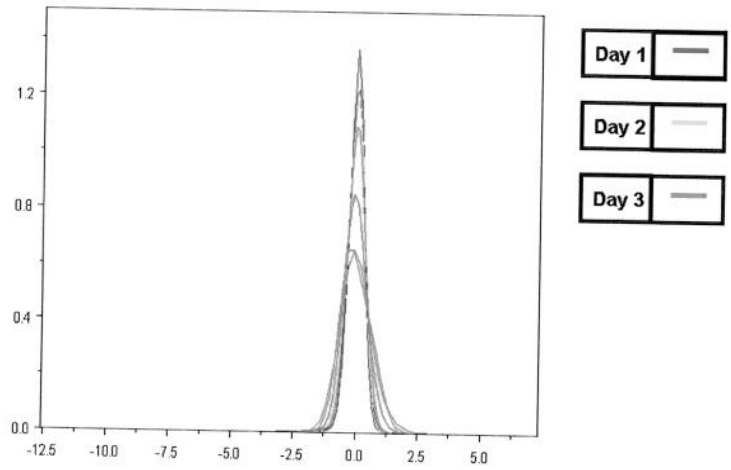

c

Fig. 22. Density plot of all normalized ratios for liver samples. Day 1 samples are represented by the green plot, day 2 samples are represented by the yellow plot, and day 3 samples are represented by the red plot.

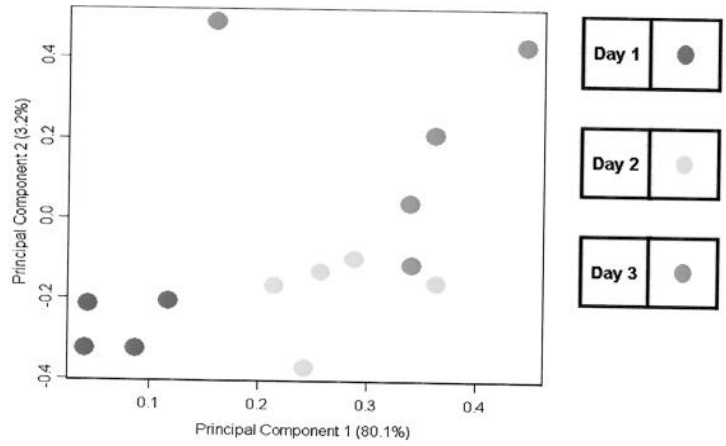

a

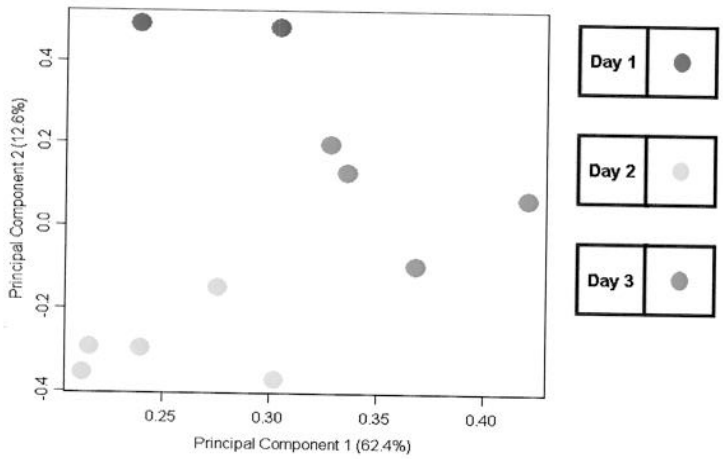

b

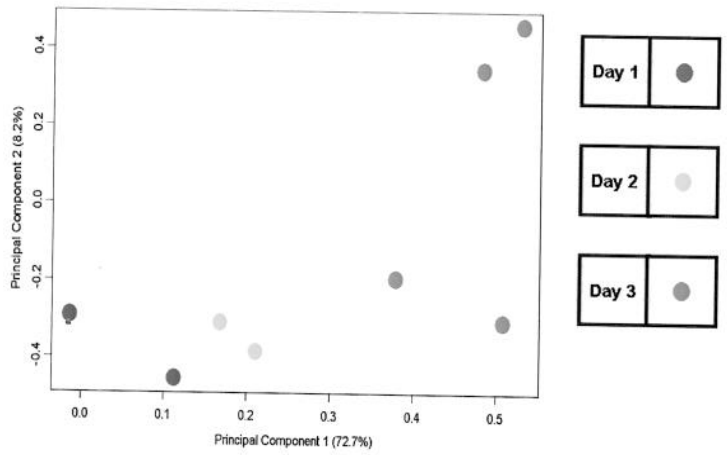

c.

Fig. 23.Covariance principle component analysis of liver samples using normalized ratios for all genes. Day 1 samples are represented by green dots, day 2 by yellow dots, and day 3 by red dots.

Lung

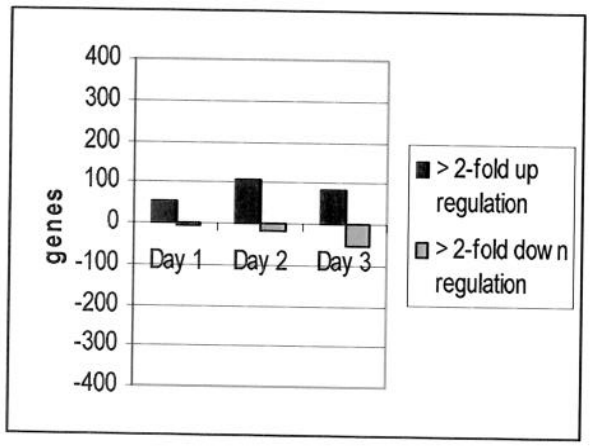

Spleen

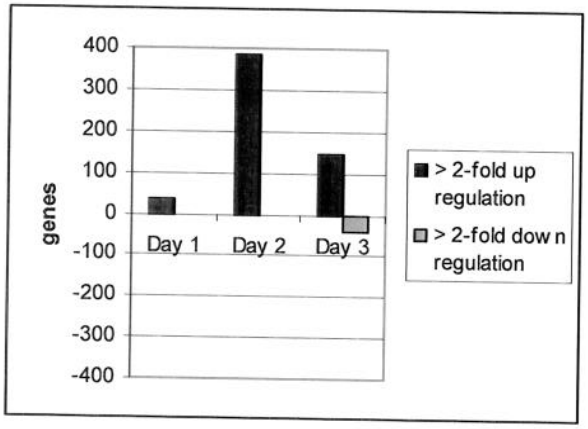

Liver

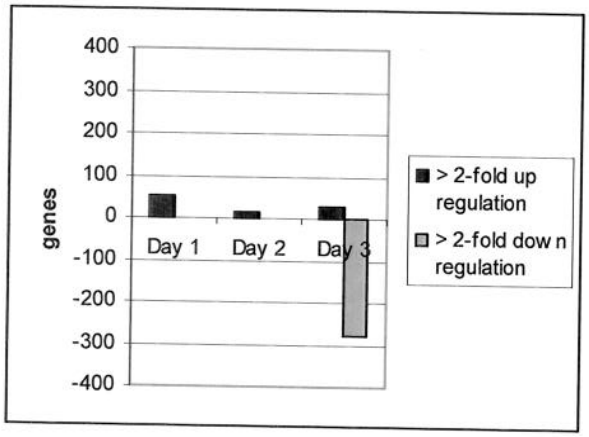

Figure 24. Genes significantly up- (positive on the y-axis) or down- (negative on the y-axis) regulated during anthrax disease progression.

Lung

Day 1 (242)		Day 2 (1080)		Day 3 (1572)	
FC	Frequency	FC	Frequency	FC	Frequency
-4	0	-4	73	-4	127
-3	0	-3	136	-3	142
-2	29	-2	321	-2	278
-1.5	193	-1.5	324	-1.5	414
1.5	0	1.5	0	1.5	0
2	14	2	226	2	599
3	4	3	0	3	12
4	1	4	0	4	0
More	1	More	0	More	0

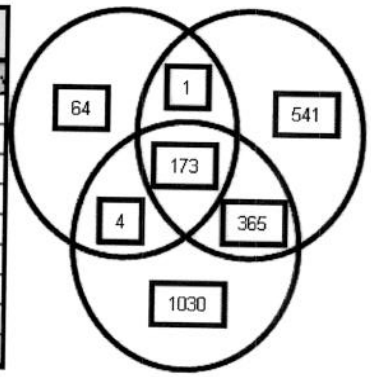

Spleen

Day 1 (100)		Day 2 (821)		Day 3 (544)	
FC	Frequency	FC	Frequency	FC	Frequency
-4	9	-4	0	-4	4
-3	12	-3	17	-3	25
-2	26	-2	265	-2	163
-1.5	44	-1.5	536	-1.5	275
1.5	0	1.5	0	1.5	0
2	9	2	3	2	75
3	0	3	0	3	2
4	0	4	0	4	0
More	0	More	0	More	0

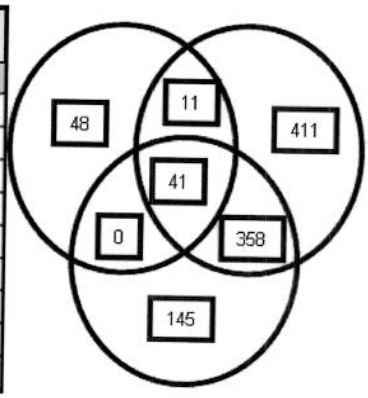

Day 1 (19)		Day 2 (105)		Day 3 (1383)	
FC	Frequency	FC	Frequency	FC	Frequency
-4	0	-4	0	-4	4
-3	0	-3	1	-3	12
-2	0	-2	12	-2	25
-1.5	10	-1.5	63	-1.5	300
1.5	0	1.5	0	1.5	0
2	9	2	29	2	943
3	0	3	0	3	99
4	0	4	0	4	0

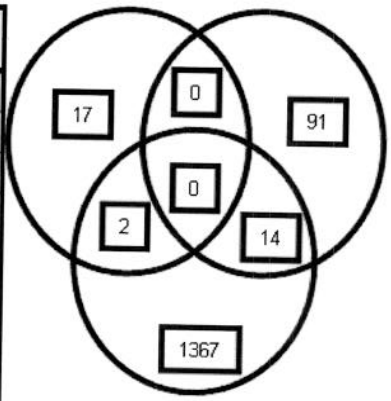

Liver

Figure 25. Number of genes with significant expression changes in the murine organs. Sample values are considered significant if their p-values are < 0.05. A ratio is considered 'changing' if it is > or < 1.5 from normal expression of 1. Circles corresponds to days 1 to 3 (clockwise), and overlapping sectors indicate numbers of common genes. FC, fold change.